Propulsion System Design for an Unmanned Underwater Vehicle (UUV)

Author

SHAHBAZ ALI

Regn Number

00000277895

Supervisor

Dr. SAMIUR REHMAN SHAH

DEPARTMENT MECHANICAL ENGINEERING

SCHOOL OF MECHANICAL & MANUFACTURING ENGINEERING

NATIONAL UNIVERSITY OF SCIENCES AND TECHNOLOGY

ISLAMABAD

DECEMBER, 2021

Propulsion System Design for an Unmanned Under Water Vehicle (UUV)

Author

SHAHBAZ ALI

Regn Number

00000277895

A thesis submitted in partial fulfillment of the requirements for the

degree of

MS Mechanical Engineering

Thesis Supervisor:

Dr. SAMIUR REHMAN SHAH

Thesis Supervisor's Signature: _____

DEPARTMENT MECHANICAL ENGINEERING

SCHOOL OF MECHANICAL & MANUFACTURING

ENGINEERING

NATIONAL UNIVERSITY OF SCIENCES AND TECHNOLOGY,

ISLAMABAD

DECEMBER, 2021

Declaration

I certify that this research work titled "Propulsion System Design for an Unmanned Under Water Vehicle (UUV)" is my own work. The work has not been presented elsewhere for assessment. The material that has been used from other sources it has been properly acknowledged / referred.

Signature of Student

SHAHBAZ ALI

2018-NUST-MS-Mech-00000277895

Certificate for Plagiarism

It is certified that ~~PhD~~/~~M.Phil~~/MS Thesis Titled "<u>Propulsion System Design for an Unmanned Under Water Vehicle (UUV)</u>" by <u>Shahbaz Ali</u> has been examined by us. We undertake the follows:

a. Thesis has significant new work/knowledge as compared already published or are under consideration to be published elsewhere. No sentence, equation, diagram, table, paragraph or section has been copied verbatim from previous work unless it is placed under quotation marks and duly referenced.

b. The work presented is original and own work of the author (i.e. there is no plagiarism). No ideas, processes, results or words of others have been presented as Author own work.

c. There is no fabrication of data or results which have been compiled/analyzed.

d. There is no falsification by manipulating research materials, equipment or processes, or changing or omitting data or results such that the research is not accurately represented in the research record.

e. The thesis has been checked using TURNITIN (copy of originality report attached) and found within limits as per HEC plagiarism Policy and instructions issued from time to time.

<u>**Name & Signature of Supervisor**</u>

<u>Signature</u>**:**

Copyright Statement

Acknowledgements

Dedicated to my wife whose tremendous support and cooperation led me to this wonderful accomplishment.

Abstract

Unmanned underwater vehicles are small submersible platforms, commonly used by developed nations for military and commercial purposes. The powering of UUV is one of the most important factors as it consumes a high proportion of the weight and space available in a submersible platform. Approximately, 35% of weight and 50% of the total volume is devoted to energy storage and powering of propulsion system. The emphasis of this research is to find propeller with suitable diameter, no of blades at a location so to minimize the powering requirements of DARPA SUBOFF UUV. Initially, coefficients of drag and resistance was calculated using ITTC guidelines. Wake survey of the tail/stern of DARPA SUBOFF UUV was carried out using COMSOL MULTIPHYSICS 5.6. Utilizing this analysis 07 x different locations were marked for further analysis with 02 x different propeller diameters and 02 x different propeller blade configurations. The analysis of these 28 x combinations resulted in determination of a plane where minimum powering requirement has arrived with suitable propeller diameter and optimum number of blades.

Key Words: *DARPA Suboff, Propulsion System, UUV*

Table of Contents

List of Figures

List of Tables

CHAPTER 1: INTRODUCTION

Unmanned Underwater Vehicles (UUV) are currently being developed at large scale. Almost all the developed nations are working to develop submersible platforms that can be remotely operated through fiber optic cable without endangering human life. These platforms can be operated autonomously using Artificial Intelligence to conduct research, reconnaissance or military activity.

The motive behind the development of UUV platforms was to conduct ocean research. Since, average ocean depth is around 04 km's [1] therefore it was too risky to send human at such depths. Initially, an autonomous underwater vehicle was developed for use of University of Washington to conduct the research in Antarctic regions.

During cold war era Russians developed a UUV [2] that was solar powered and has the capability to do operations for longer time. This started a race between leading submarine developing nations.

Currently, UUVs, as shown in fig 1 below, are being used for mine countermeasure's operations, oceanography, research, rescue and intelligence gathering. One important parameter that describes the ability of platforms is the propulsion system i.e. the velocity at which these UUVs can operate.
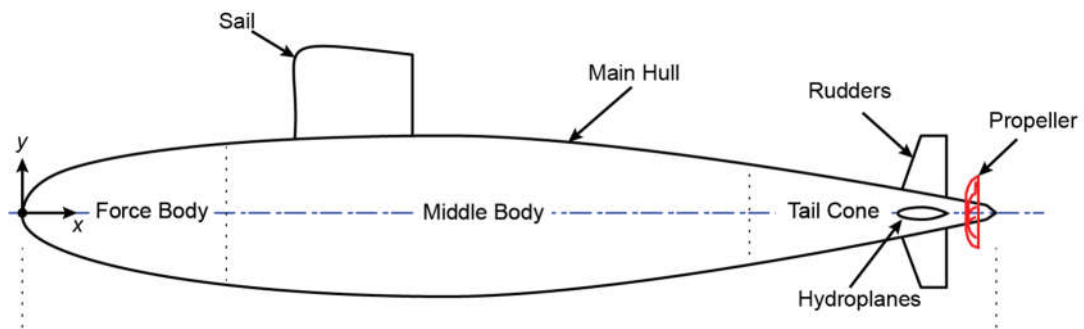
Figure 1: UUV

The powering of an unmanned underwater vehicle is a design process to store energy efficiently and later convert it to usable power. Since, up to 50% volume of any submersible [3] is occupied by energy storage. Propulsion system design thus requires such design techniques which enhances the underwater endurance of the submersible platforms by utilizing efficient propulsion systems.

Maximum speed of the UUV determines the size of the energy bank required for propulsion, it is the time at speed which governs the energy storage capacity requirements of a submersible

In order to have an efficient propulsion system there are four desirable features which a UUV should have:

- Appended Hull drag with low resistance value
- Propulsion mechanism with relatively high efficiency
- Propulsion plant with high efficiency values
- Enhanced energy storage capacity.

Classification of marine platforms and

Water-born vehicles can be classified into two main groups, namely ships or surface platforms and submersibles or sub surface platforms. Merchant ships are used to transport passengers and goods and can be further categorized into cargo and passenger ships. Military ships, on the other hand, are used for defense purpose and are dedicated to protecting the country from hostile intruders. Aircraft carriers, destroyers, corvette, frigate and cruiser are main types of naval vessel. Subsurface platfroms can broadly categorized as manned or unmanned platforms both of which are being used for military and research/rescue missions.

Classification of Propulsion System

Propulsion system for UUVs is a mechanism installed at aft of the marine platform, used to produce thrust in order to push the vessel through water. The basic physics of propulsion system remains same for ships and submersible crafts.

Initially steam turbines were used to power propulsion system of ships. It has almost been replaced by diesel engines, nuclear power plants for ships as well as submarines. However, few ships are

using gas turbine power plants and some platforms are being powered by liquefied natural gas (LNG) as a better option due to marine emission.

Air independent propulsion (AIP) systems are common on submarines to increase submergence endurance. Fuel cells, MESMA, nuclear reactor and closed cycle diesel engine are prime mover in AIP propulsion system.

First submersible was human powered, however in modern times, human propulsion can only be found on small boats as auxiliary propulsion. Human propulsion has now been replaced by mechanical propulsion. Most watercraft are now energized by diesel engine and propelled by screw propeller.

Propulsion system can be mechanical, electrical or hybrid, depending on the mission profile of a platform and magnitude of auxiliary load. Submersible platforms can be battery driven i.e. batteries connected to the motor which ultimately rotates the propeller. Keeping the complexities and maintenance schedules, Mechanical systems are installed on manned submersibles.
Hybrid propulsion system is a combination of both electrical and mechanical propulsion systems and is useful when auxiliary load is only a fraction of total propulsive power and the platform is mostly to be sailed at low speed.

Energy source for most of the present UUVs is based on high energy density batteries that provide enough endurance which is necessary to conduct the designated mission.

Main parts of propulsion system

Marine propulsion system is mainly composed of three components or sub-systems namely
Prime mover,
Propulsor (propeller)
Transmission system.

Prime mover in case of a UUV is mostly a cluster of high energy density batteries, since UUVs nowadays are compact in size, therefore placement of an internal combustion engine can some

times become bigger problem due to addition of multiple auxiliary systems like supply of sea/fresh water for cooling circuit, lubrication, greasing, exhaust management system and many more.

Propulsor works on Newton third law of motion as it pushes water in backward direction and gets a forward reactive force called thrust. Different types of Propulsor are currently being used, including pump jets, water jets, propellers or thrusters.

Propeller is selected in term its type (CPP or FPP), diameter , number of blades , blade area ratio, pitch ratio and, last but not the least, design RPM. Number of propeller blades depend on the load and material of the blade [4]. Smaller is the number of blades, higher will be the propeller efficiency but it can also cause hull induced vibration.

Maximum practicable diameter and smallest propeller RPM will give maximum efficiency and better cavitation performance [5]. Blade area ratio can be used to decrease cavitation. Keller method is used to calculate minimum acceptable blade area ratio, while Burrill method is used to calculate or blade area ratio for allowable back surface cavitation. Propeller is more efficient at a value of pitch ratio called optimum pitch ratio.

Propeller design is usually faced with conflicting boundary conditions. Aim of the design is to select or design most efficient propeller with minimum noise, vibration, cavitation and structural integrity. Propeller efficiency is limited by the largest propeller diameter and smallest propeller RPM. Largest propeller diameter is restricted by the wake field at the aft of platform. Hull induced vibration can also be decreased by increasing number of blades at the cost of propeller efficiency. Therefore, a balance amongst all these conflicting parameters is required.

Minimum blade thickness at 0.25R and 0.6R is given by Chinese classification society (CCS) [6]. Propeller efficiency can be increased by using high strength material. Because high strength material will require less blade thickness and hence the drag can be decreased by using high strength material.

Optimum propeller parameters are calculated by plotting and superimposing thrust curve of ship on propeller open water diagrams. Optimum propeller RPM, pitch ratio and efficiency at the intersection of ship and propeller thrust curves, also known as propeller operational point, are calculated.

Propeller open water diagrams are now arranged in a more meaningful forms called propeller coefficient charts. In propeller coefficient charts, after calculating Taylor's coefficient, propeller efficiency, pitch ratio and advance ratio is calculated at the intersection of Taylor coefficient and maximum efficiency line. Two types of coefficient charts i.e. B_{p1}-δ and B_{P2}-δ are in common use depending on available data.

To decide whether a fix pitch propeller (FPP) or controllable pitch propeller (CPP) is to be used depend on the mission or operating profile of the platform. If a dominated has dominated design conditions, then FPP is recommended. Moreover, if the UUV has to operate in off-design conditions most of the time or have multi-off-design conditions, then CPP, with hybrid propulsion system, is the most viable option [7]. CPP enable propulsion system to provide variable thrust at constant RPM, which is pre-requisite for a constant voltage and power to the platform grid.

Highly efficient propulsor at reasonable and acceptable cost is chosen in order to minimize the machinery power, cost and improve fuel economy. Single screw propeller is the best option as for as the efficiency is concerned. But reliability, availability redundancy, maneuverability, speed, and required thrust dictates the use of more than one propeller.

CPP has several advantages over FPP, like better maneuverability, no need of reduction gear box and, more importantly, the adaptability of propeller pitch to match/optimize propeller with the energy source even in extreme off-design conditions. On the other hand, CPP is vulnerable to damage due to internal pitch mechanism. CPP is best suited, when PTO is installed without frequency convertor.

Efficiency of CPP is less than FPP due to its large hub size. Also, drastic decrease in efficiency and pressure side cavitation is observed at extremely reduced pitched operation [8]. At given

propeller revolution rate, increasing propeller pitch will result in suction side cavitation. On the other hand, decreasing propeller pitch beyond certain limit will cause pressure side cavitation.

Propulsion system, with CPP, is more responsive and maneuverable than system with FPP. Because changing thrust, with either using gear box or firing order in case of reversible engine, will take some time to be effective. CPP, due to its pitch adaptability, make it possible to absorb full power at bollard pull and at free running condition.

CPP, although, increases the degree of complexity as compare to FPP. But on the other hand, it has some advantages. Direction of platform motion can be reversed by reversing rotation of the propeller without gearbox. Similarly, thrust control can be improved without increasing or decreasing propeller rotational speed. CPP is, sometimes, preferred despite of its poor efficiency, particularly, in confined water conditions or to match energy source characteristics, which is designed to best run at one speed all the times.

Efficiency is least affected by the skew angle of propeller, but it reduces hull induced vibration, unsteady propeller induced pressure forces & moments and cavitation. On the other hand, it decreases backing efficiency and difficult to manufacture. Very high skew is not always beneficial for surface platforms but highly skewed propellers are required for military class submarines [9]. However, for UUVs moderate to high skew is preferable.

For surface platforms, a propeller is usually raked aft (5º to 6º) to increase tip clearance thus reduces hull induced vibration. Ships with highly loaded propellers, like tug boats, are shrouded to prevent propeller ventilation and increase propeller thrust due to nozzle effect.

FPP screw propellers are used for most of the UUVs naval and commercial platforms due to reliability. Accelerating ducting propellers are more efficient than decelerating ducting propellers due to increase of pressure in the decelerating ducting propellers.

Water jet Propulsor are in use since 1954 due to its noise-free and high-speed performance. Contra-rotating propellers, two separate propellers are attached to two separate but co-axial shafts to take advantage of slipstream. Contra-rotating propellers are mostly used in Torpedoes.

Transmission system in mainly composed of shaft, bearings, stern-tube and supporting brackets. Gear box if used, is for reducing prime mover speed to propeller speed, reversing direction of propeller rotation and to couple multiple engines to one propeller or vice versa.

Stern tubes and shaft bearings are used to pass propulsion shaft through hull of the UUV. Most of the today's stern tubes are sea water cooled.

With the advancement of technology, modern UUVs are using thrusters for propulsions. Thrusters provide a quick solution as they have a shrouded propeller attached to motor through shaft. This compact propulsion solution has helped to reduce the size of platform as energy source consumes 40% of the UUVs weight and space

The flow into any propulsor will alter its efficiency and acoustic performance. Shape of hull especially the forward dome and tail cone angle; the casing; the sail; and the aft appendages all have a influence over this. There will be an irregular wake field into the propulsor depending on the sail configuration and aft control surfaces as shown in the figure 2 below. As a result, forces will fluctuate, creating vibration and noise.
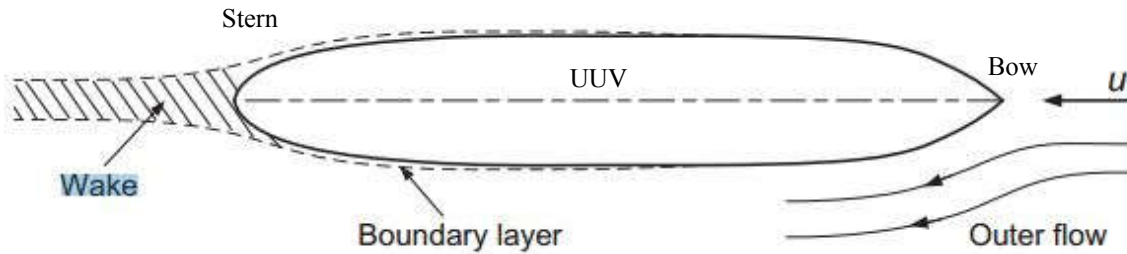
Figure 2: Wake Field around a UUV

Presence of propeller behind a submersible creates thrust, but the presence of this propeller also caused a drag. This drag due to presence of propeller is labeled as thrust deduction fraction. This fraction of thrust deducted is a function of tail cone angle and ratio between propeller diameter to hull diameter.

The hull efficiency is the ratio of effective power to thrust power. It is possible to evaluate thrust power. The drive train of a UUV has been explained in figure 3 below.

Effective Power (P_E): Power required to tow a platform (without propeller) in calm waters at defined speed
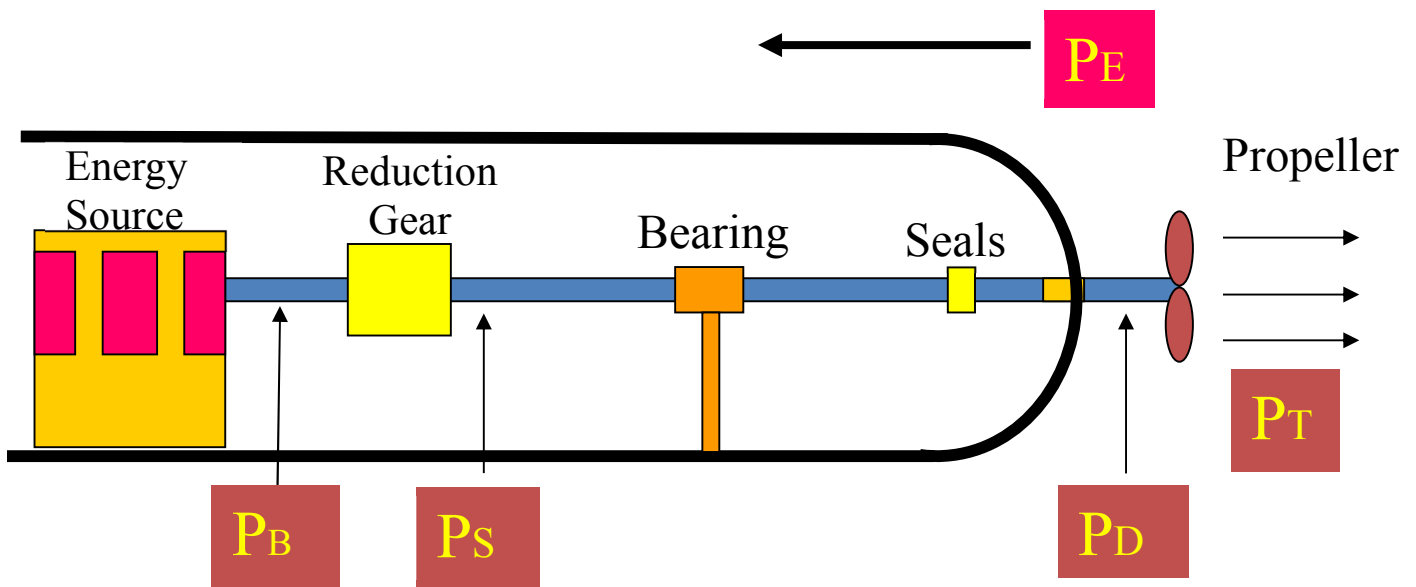
Figure 3: UUV Propulsion drive-train

Brake Power (P_B): Power coming out of an engine or power output of an energy bank in case of UUVs

Shaft Power (P_S): Power output at the shaft coming out of the reduction gears

Delivered Power (P_D): Power delivered to the propeller, the difference between shaft power and delivered power is the losses occurred at bearings and shaft seals

Thrust Power (P_T): Power created by propeller to generate the required thrust; this is the result of all powers in a drive train, designed to move the platform while delivering the power to propeller

CHAPTER 2: LITERATURE REVIEW

Published Research

Poul Andersen et al (2009) [10] elaborated how propulsion system designing for a submersible platform is different from that of a surface ship due to stringent requirements of cavitation noise for a submarine propeller. His work explains the significance of wake field in propeller designing. Wake filed of a U-boat shows the wake high and low weak regions along the circumference.

A comparison of acoustic noise between a 07 x blade propeller and 08 blade propeller has been conducted experimentally. For this purpose, 04 x different propellers (kappel type) were designed and tested in cavitation tunnel. Results showed that 08 bladed propellers has less acoustic signature in comparison to 07 bladed propeller.

Flood et al. [11] took a propulsion system designed for a sea going platform to analyze its behavior in off design conditions. He used MATLAB codes employing Lerbs method for accurate modeling of circulation distributions and induced velocities for a wide range of operating conditions.

MATLAB developed code give an insight to output of changes made during design stages. Finally, the results were found to be in good agreement to propeller open water diagram.

Nathan Chase and Pablo M. Carrica [12] performed computation and validation for self-propulsion of the appended DARPA fitted with INSEAN E1619 propeller located at x/L 0.975. CFDShip lowa (v4.5) was used with DDES approach. Results showed that propeller performance matches experimental data

Zhang Li et al [13] performed propeller hull interaction with a five bladed propeller, attached to hull of DARPA Suboff, for powering performances of submarine. Thrust identity method was used to analyze the self-propulsion factors. Moreover, this study found that effect of free surface is mainly due to the sail of platform and these free surface effect (wave making resistance) almost diminish when a submarine is at a depth equal to 1/3 of its total length.

Yasmein Ozdan [14] conducted numerical analysis of tail cone angle effects on hull efficiency of DARPA Suboff fitted with INSEAN E1619 propeller. Tail cone with 04 different cone angles were analyzed numerically using ANSYS-FLUENT. It was found that resistance of platform increase.

However, wake fraction and thrust deduction decreases with an increase in the tail cone angle. Hull efficiency and propulsive efficiency increase to some point and then decreases with an increase in tail cone angle.

Florain et al. [15] presented a comparison on four different set of algorithms and optimization techniques for optimization of propeller parameters. In the process he used 07 different propellers.

Starting with the traditional manual propeller designing concept to formulation of automated designing process with built-in optimization tools. Author proves with help of test cases that automated propeller designing is a fast method.

M Cansin et al. [16] has calculated the propeller noise numerically to predict the acoustic signature and minimize the radiated noise levels of a DARPA Suboff attached with INSEAN E1619 propeller .

Propeller flow envelop is assessed with CFD employing URANS, and hydro-acoustics are analyzed using Ffowcs-Williams and Hawkings equation. Wake was imposed, but it did differed significantly.

A Posa & E Balaras [17] conducted numerical investigation of wake for DARPA Suboff. It is shown that the wake of the body is affected mainly by the shear layer from the trailing edge of the fins and the turbulent boundary layer growing along the stern, while the influence of the wake of the sail is minimal

Moonesun M, et al. [18] studied the behavior of a model submarine in submerged conditions at a towing tank and compared these results with CFD results of same platforms. Four different formula-based techniques have been introduced to fine submerged resistance.

D.V Efrov et al. [19] experimentally analyzed the free surface effects for submarine operating in shallow waters. 03 different depths were marked initially. It was concluded that the yaw rate decreases uniquely to zero as in case of yaw to yaw motion is critically damped.

Thanh-Long Le [20] has used a torpedo shaped body to perform hydrodynamic analysis using COMSOL Multiphysics. It was found that torpedo experiences max pressure at its nose section. Increase in Drag and lift values are driven directly by increase in velocity

Faizal et al. [21] analyzed drag regime around a marine riser using k-epsilon turbulence model in COMSOL Multiphysics. Results showed that coefficient of drag is a function of Reynolds number as coefficient of drag dropped in line with experimental data published by Marin Netherlands.

Leksono et al. [22] did propulsion system designing for a 22m long midget submarine. Lines plan of the platform was published using data from a similar platform. Required thrust and Thrust horsepower was calculated using Virginia technology method which is in line with ITTC guidelines.

Platform had cruciform hydroplanes at aft, therefore a bladed propeller with diameter range of 0.4 to 0.6 was assessed and finally a B-series (B7-85) was recommend for that specific platform

S. Sezen et al. [23] determined the self-propulsion characteristics of DARPA Suboff using 07 bladed INSEAN E1619 propeller installed at the tail location of x/L 0.978. Resistance, self-propulsion and Open water characteristics of propeller were determined through CFD using RANS method.

Wake survey of the DRAPA Suboff tail region has been conducted thoroughly. As a first step, Actuator disc theory has been applied i.e. an infinitesimal thin sheet with diameter equal to that of

propeller is with infinite number of blades is used to calculate self-propulsion point, later moving reference frame technique was used to simulate the actual propeller.

Results were validated by comparing with the experimental data and CFD results published by previous researchers.

Delen C, et al. [24] determined the hydrodynamic performance parameters of DARPA Suboff attached to a DTMB-4119 propeller located at x/L 0.987. Resistance values were determined for 02 x different velocities and were found to be aligned with experimental data. It was concluded that the application of Actuator Disc Theory is beneficial in terms of computational cost and time.

Sekan Ekinci [25] present a practical approach for design development of propeller that has least chance of mistakes encountered during reading of propeller open water diagrams. 03 x different b-series propellers cases have been presented and results shows that author approach of using model series data based on experiments remains the most relevant technique.

Andrea Pecoraro et al [26] determined the flow behavior at aft of a chemical tanker. Detailed velocity survey was conducted using Laser Doppler velocimetry These tests were conducted with and without propeller configurations.

This study recommended to increase the skew angle of propeller blades to avoid harmful effects of propeller wake.

Peng Han et al. [27] simulated flow around hull form of DARPA Suboff..Three different fillets were attached with the sail and hydroplanes of platform to asses the effect on horseshow vortex production and intensity. Results shows that convex type of fillets decrease this horseshow effects and the flow at propeller plane was more smoothed.

Omer K et al. [28] determined the self-propulsion characteristics of DARPA Suboff and two surface platforms. Wake behavior of the platforms were assessed at different velocities and it was found in line with the published data.

Mashud K, et al. [29] presented study regarding flow behavior around hull of surface platforms using RANS method in Shipflow software for CFD analysis. Wake coefficients of two modern benchmark ship hulls with and without rudder-propeller interaction were assessed, and accordingly hull-propeller interactions were investigated. Results suggested a design improvement in rudder angles for a better hull-propeller efficiency.

Uzan D et al. [30] investigated the fouling effects on powering of submarines using RANS based CFD model The DARPA Suboff platform is divided in four scenarios to assess the impact of fouling at bow, stern, parallel middle body and full platform. It was found that roughness has significant impact on powering, especially if it takes place at bow of the submarine.

Ruben J. et al [31] numerically investigated the flow around DARPA SUboff 5470 and Type 209 submarines, using OpenFOAM v3.7. The purpose was to establish a location where electromagnetic speed log/ probe device can be installed. Analysis suggest that probe should installed at acceleration region i.e. one on the port/stbd side of platform and not at sail or upper deck.

Savas Sezen et al. [32] investigated the scale effects between model scale and full-scale hull form resistance and propulsion parameters for DARPA submarine. This research investigated the application of 1978 ITTC guidelines for performance prediction of submarines. It was found that full scale total resistance coefficients increase. Wake velocities were high for full scale comparatively. This study proves that 1978 ITTC performance prediction method can be applied to submarines as well.

Salimzhan A et al. [33] gave a brief overview of evolution of unmanned underwater vehicles. For the last twenty (20) years, Underwater vehicles have evolved their bulkier design and sensitive gadgetry installed for ocean research to solve theoretical and practical problems in ocean research, including commercial and military applications. The load consequently, has increased capability requirements, necessities for computational capabilities, autonomous and acoustic requirements have grown in preparation for such devices. Low cost and versatility are crucial in this case.

Finally, review of this paper reveals how underwater vehicles have developed from the very beginning to the current configurations.

In the light of research on development history of UUVs author envisions the future trends in design and development will include using new materials, new propulsion systems with high energy banks, increase in military application, UUV miniaturization, reducing UUV design and development costs and lastly the use of artificial intelligence.

Overview of Propulsion Theories [34]

Conventional theories behind the propelling action began to develop at the second half of the nineteen century. The most notable work was the momentum theory of Rankin, which was later extended and followed by the blade elements theory, proposed by Froude.

Modern theories to describe propelling action were formulated by Lanchester and Kutta at the beginning of nineteen century. The idea to relate the circulation with lift was first presented by Lanchester and Kutta. Mathematical equation to relate the two parameters was later given by Joukowski in 1996.

Prandtle was the first who presented the classical lifting line theory. Prandtle was of the view that lift of a wing is due to circulation of flow around its body. Munk, on the other hand, first introduced the concept of "induced drag" and presented aerofoil theory which yielded exceptionally good results at wide range of subsonic flow.

The theories discussed above were later converted into some mathematical functions, aimed to predict the behavior and performance of propeller.

Rankin in 1886, developed a theory based on axial flow of water across the disc. Rankin theory was unable to design blade geometry because he did not consider the propeller geometry. The theory assumed that the flow across the propeller is inviscid and that the propeller can be replaced by a hypothetical disc having same diameter as that of propeller but with infinitesimal thickness.

The disc assumption lead to infinite number of propeller blades and thrust generation without any rotation. The plate is assumed to relate to the engine and delivered power to the water because of pressure differential across the two planes of plate.

R.E Froude in 1887, developed, based on Rankin work, a more practical model by allowing rotation flow across the imaginary disc. The theory is known as general momentum theory. In both these models, the delivered power is calculated based on the change in kinetic energy.

The work of Rankin was further modified by W Froude in 1878 by considering the blade geometry and is, therefore, named blade element theory. W. Froude divided propeller blade into large number of elementary strips that can be regarded as an aerofoil.

This theorem was, although, very comprehensive but failed to yield the desired accuracy of results due to some computational complexity. The theorem was also unable to accurately predict the performance of propeller. Still it was a foundation for all theories thereafter.

Before 1930, the propulsion system design was developed along two separate lines i.e. momentum theory and blade element theory. The two theories give inconsistence and impractical results in some respects.

For example, the momentum theory, which was based on viscous fluid, gave 100 percent efficiency if viscous effects are ignored. While blade element theory gives some range of propeller efficiency depending on speed of advance and torque coefficient. Later, the two approaches were combined but still it was not entirely satisfactory.

A theory for model propeller with zero boss radius was formulated by Goldstein. Later, the work of Goldstein was modified, and a detailed calculation was made for 3 to 6 bladed propellers having a finite hub radius by Tachmindji and Milam.

With the theories of Goldstein, Betz and Prandtl and Lanchester, a basic building block, for more practical rotational propeller theory, was prepared before 1930.

Burrill in 1944 was first, who devised the most comprehensive and coherent procedure for propeller calculation. Burrill, basically, combine the basic principles of momentum and blade element theory, keeping in view the vortex analysis approach.

The method gave very accurate and reusable results for moderately loaded propeller operating at near design conditions. On the contrast, the method was failed to yield accurate results for light or heavy loaded propeller. Burrill theory, in true sense, was the final attempt to blend the momentum and blade element concepts.

Lerbs in 1952 developed a technique based on lifting line concept for moderately loaded propellers operated in inviscid working fluid. The assumption of moderate loading allows the effect of induced velocities and as result the vortex sheets originating from each blade differ slightly from the actual helical form.

The latter assumption is only valid for lightly loaded propeller. The model presented by Lerbs was considered at that time classical representation of the lifting line concept. For wake estimation, the propeller is assumed to operate in a wake field that is considered constant circumferentially and varies radially.

The lifting line method, based on lifting line theory, is a purely mathematical approach to compute the lift of a wing or blade of propeller.
Eckhardt and Morgan proposed an approximate design method based on the assumptions that propeller action does not contract the slip stream and normality of induced velocity prevail.

These two assumptions confined this method only to light and moderately loaded propellers. In this method, the open water and wake adapted propeller are separately treated with the open water case as the solution of wake adapted propeller.

The lifting surface method was modified and extended by Kerwin, later, named as vortex lattice method. The lifting lattice method is basically a numerical technique used in CFD, mainly in the early stages of aerofoil design.

The model regards the lifting surface or aerofoil as a thin sheet of discreet vortices, in contrast to lifting line method, which is based on only one vortex, to calculate the required lift and drag, without taking the effect of thickness and viscosity.

This method faced two difficulties i.e. the localized error at or near the leading edge and the widespread error at or near the closely packed and thick section of blade root. These two difficulties are overcome in the most recently devised method known as boundary element method.

This method was originally pioneered for aircraft industry, but later in 1980, the application of this method was extended to marine applications. This method gave quite satisfactory results, then conventional lifting surface method, as for as the blade pressure distribution and open water characteristic are concerned.

As this method uses computational or computer codes to calculate propeller parameters. Kinnas in 1992, had developed some boundary element computer codes, based on boundary element method, to solve unsteady cavitating flow around propeller blades.

Subsequently, the approach has been further modified to include the effects of non-cylindrical hubs, mid-chord surface cavitation etc. The results obtained were in very close correlation with experimental results.

During the last ten to fifteen years, a considerable work has been done on the application of computational fluid dynamics on the design and analysis of marine propellers. This technique has now reached to a level where one can get very useful and meaningful insight into the complex three dimensional, viscous and cavitating flow across the propeller.

While a lot of work is still in progress to generate more comprehensive and robust computer codes, still these techniques have not yet reached to the level of widespread acceptance. But definably, this will happen in near future. Different modeling approaches, so far, has been formulated to analyze the flow around cavitating and cavitation free propellers.

These include Reynolds average navier-stoke (RANS) method, large eddy simulation (LES) technique, detached eddy simulation (DES) and direct numerical simulation (DNS).

These methods are considered excellent tools for research work, but for practical propeller design these methods still have limitation due to computational effort in term of time and high-speed computer.

Propeller open water diagrams and propeller power coefficient charts are now-a-days used for propulsion system design and analysis. Propeller open water diagrams are used for academic studies, while propeller coefficient charts are used for practical design.

These two charts are based on some regression analysis on the model testing results, on a propeller whose material and geometry may be different from any propeller under consideration. Therefore, the result may be erroneous due to reasons**.**

A more accurate method is to perform model testing for design and analysis of propulsion system. This technique is very helpful to, especially, calculate the unsteady and inhomogeneous wake behind the hull surface.

The extrapolated results are, somehow, erroneous due to scaling effects and failure to fully establish all similarities, between model scale and its full-scale counterpart, in true sense. The model testing is also an expensive technique but are in common use for practical design.

Propulsion system matching is required to ensure optimum utilization of engine power and RPM. Propulsion system matching is basically a two steps process. In first step, ship resistance and propeller thrust are balanced, while in second step propeller and engine powers are conserved.

Propeller open water diagrams and propeller coefficient charts are used depending on the available data. Propeller demand curve is plotted and combined with engine operating envelop. For optimum propulsion system, the propulsion MCR point must coincide with either engine MCR point or lies at or near the point of minimum fuel oil consumption.

Design of efficient propulsion system mainly depends on the selection of optimum and cavitation free propeller.

Optimum propulsion system will decrease the required propulsion power and, thereby, decreasing size of engine or initial cost of propulsion system. This will result in decease fuel consumption and subsequent exhaust emission from engine. Cavitation, beyond certain limit, will generate noise, erode the propeller and will result in hull induced vibration.
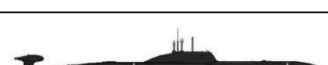
Parametric Study [35]

In addition to literature review, a parametric study was performed to observe the location of propeller installed with world modern attack submarines as shown in figure 4 below.

Since, these platforms are currently operating around the world in different regions with different mission performance requirements. Parametric study reveals that all the platforms have different aft tail cone angles and aft hydroplanes including rudders.

However, investigation of these submarines propulsion system design reveals that different approaches have been adopted for the location of propulsors.

As it can be observed that United Kingdom (UK) designed platforms i.e. Astute class platforms

Vehicle Type	Propulsor Configuration	L (m)	Φ (m)	V (knots)
Ohio (USA)		170	13	25
Vangaurd (UK)		150	12.8	25
OSCAR-II (Russia)		155	18.2	32
Akula (Russia)		110	13.6	28
Los Angeles (US)		110	10	20
Astute (UK)		97	11.3	30

and Vanguard class submarines have their propulsors very close to hydroplanes.

Figure 4: Parametric Survey

On the other hand, Russian platforms like OSCAR-II class and Akula class have their propulsors away from rudders. Oscar-II class platforms have one exception i.e. they have two propellers attached to two different shafts.

United States of America's design philosophy is a mix basket as the OHIO class platforms have moderately far placed propeller in comparison to location of propeller for Los Angeles class submarines.

As we discussed in the beginning chapter that physics of propulsion system remains almost same. Therefore, this paramedic study necessitates propulsion system designer to understand the physics involved for better reasoning of why one propulsor is placed very close and other far away.

Research Gap

The available research is focused on optimization w.r.t self-propulsion parameters, noise prediction, hull efficiency and propeller hull interactions. However, literature lacks quantification of propeller location effects on powering requirements.

Therefore, literature fails to suggest the optimized location for propeller Consequently, during the preliminary design stage the optimum location of the propeller is not available on hand. This could lead to inefficient designs thus resulting in low endurance for submerged platforms

Foregoing discussion necessitates the analysis for effects of propeller locations, as shown in fig 5, on powering requirements and propulsion efficiency for an Unmanned Underwater Vehicle (UUV)
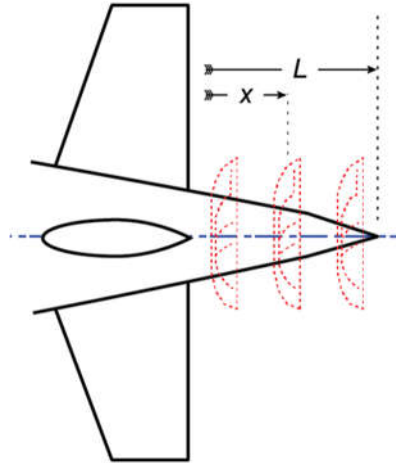
Figure 5: Propeller Location

Propellers in this picture are placed at different locations. Since, practically only one propeller must be placed at a time. So, each location of propeller can be denoted with "x" along the length where x =0 at nose and x=1 at tail.

Accordingly, throughout this research propeller location along the length of platform will be denoted a "x/L" where L is the length overall i.e. length of the platform

Objective

Therefore, this study will be focusing on following objectives:

- Quantify the resistance and the effective power (P_E) requirement for the case study platform

- Quantify the delivered power (Pd) at varying tail cone locations (x) of the propeller w.r.t. the overall length (L) of the platform.

- Compute the propulsion efficiency (η) to establish the optimized propeller location w.r.t. the overall length (x/L) through CFD simulations

CHAPTER 3: METHODOLOGY

A limited data related to submersible platforms is available in open literature. Therefore, in order to numerically investigate the hydrodynamic effects on propulsion powering, with change in location of propeller, has been carried out using a US Defense Advanced Research Projects Agency (DARPA) developed platform usually called as DARPA Suboff with an appended hulform as shown in fig 6 below

Figure 6: DARPA Suboff

Geometric characteristics along-with experimental data related to DARPA Suboff was published by Lieu and Huang [36] in 1998. The UUV has an overall length of 4.356 m. Platform hull is composed of a fore-body with length of 1.016 m, a parallel mid-body length of 2.229 m, an aft-body of length of 1.111 m, and an end cap length of 0.095m. Table 01 represents the dimensions of DARPA Suboff.

DESCRIPTION	UNIT	PARAMETER
Length overall (LOA)	m	4.356
Max. Hull Diameter, (D)	m	0.508
Surface Area (S)	m²	6.348
Volume (Δ)	m³	0.706

Table 1: DARPA Suboff Geometric Dimensions

Experimental study of DARPA Suboff was conducted in David Taylor Research Centre at USA where a series of resistance stripping tests and planar motion mechanism static tests were conducted for DARPA Suboff in a deeply submerged condition.

In order to answer the question of where to install the propeller? It was necessary to calculate the platform drag and powering requirements without propeller and then matching these with available experimental data.

Once these results are matched, 07 x different propeller locations are marked where propeller performance has been gauged through powering requirements at each location. Operational parameters set for these analyses are appended in table 02 below

DESCRIPTION	UNIT	PARAMETER
Max Submerged Velocity	Knots	18
Nominal Operating Depth	m	60

Table 2: Operational Parameters

Resistance to the motion of submersible platform has significant influence on top speed, and endurance. Additionally, high resistance will affect the acoustic signature due to increased flow noise; and the requirement for increased propulsion power to achieve a given speed

At nominal operating depth and with the maximum submerged velocity, Viscosity of water has great significance in terms of resistance to the motion of submerged platform. As during the submerged condition, all drag is due to the shear and normal force of the water by virtue of its viscosity.

The tangential force of viscosity described as viscous shear drag, this drag due to water tangential flow over the surface of the hull contributes to the resistance of the hull. This is essentially related to the exposed surface area and the velocity over the hull. Consequently, for a given volume of hull it is necessary to reduce the surface area.

Smooth surfaces, on the other hand, are necessary to prevent roughness and sharp discontinuities and to have a gently fluctuating shape so that no unfavorable pressure gradients build up, creating higher drag through separation of the flow from the hull, as seen in figure 7

The normal component of force acting on the platform's hull lowers pressure recovery due to non-viscous flow over a moving body. Although there are pressure variations between the bow and stem, the overall result is a zero force in the direction of motion in ideal non-viscous flow.

The normal component of drag force caused by viscosity produces a loss in the fluid's velocity, and although there is a pressure build up at the bow of the submarine, the equivalent pressure recovery at the stem is slowed, resulting in a net resistance in the direction of travel.

This form drag can be reduced by having extremely slowly varying sections across a long body, i.e. gravitating toward a needle-shaped body while having a high surface to volume ratio.

Figure 7: Flow behavior at aft of UUV

COMSOL Multiphysics version 5.6 has been used for numerical analysis to ascertain the hydrodynamics of DARPA Suboff at 07 x different tail locations defined as x/L. when x/L = 0 it means that propeller plane is at nose of platform and when x/L=1 it means that propeller is at the farthest point at the tail of platform.

Stipulations of International Towing Tank Conference (ITTC) [37] [38] including the 1978-performance prediction method have been used to calculate the total ship resistance, ITTC has published these procedures and guidelines as general description of an analytical method to predict delivered power and rate of revolutions for propeller driven platforms.

It is worth mentioning that in its original form resistance to the motion comprises of viscous resistance and wave resistance. Since, this study has been performed in subsurface mode of platform therefore wave making drag and air resistance have not been considered.

However, in case of surface platform or motion of UUV at surface of sea has two more components of resistance i.e. wave making resistance and resistance due to the air.

Resistance due to air directly depends on the velocity of air and direction of platform. Whereas, wavemaking

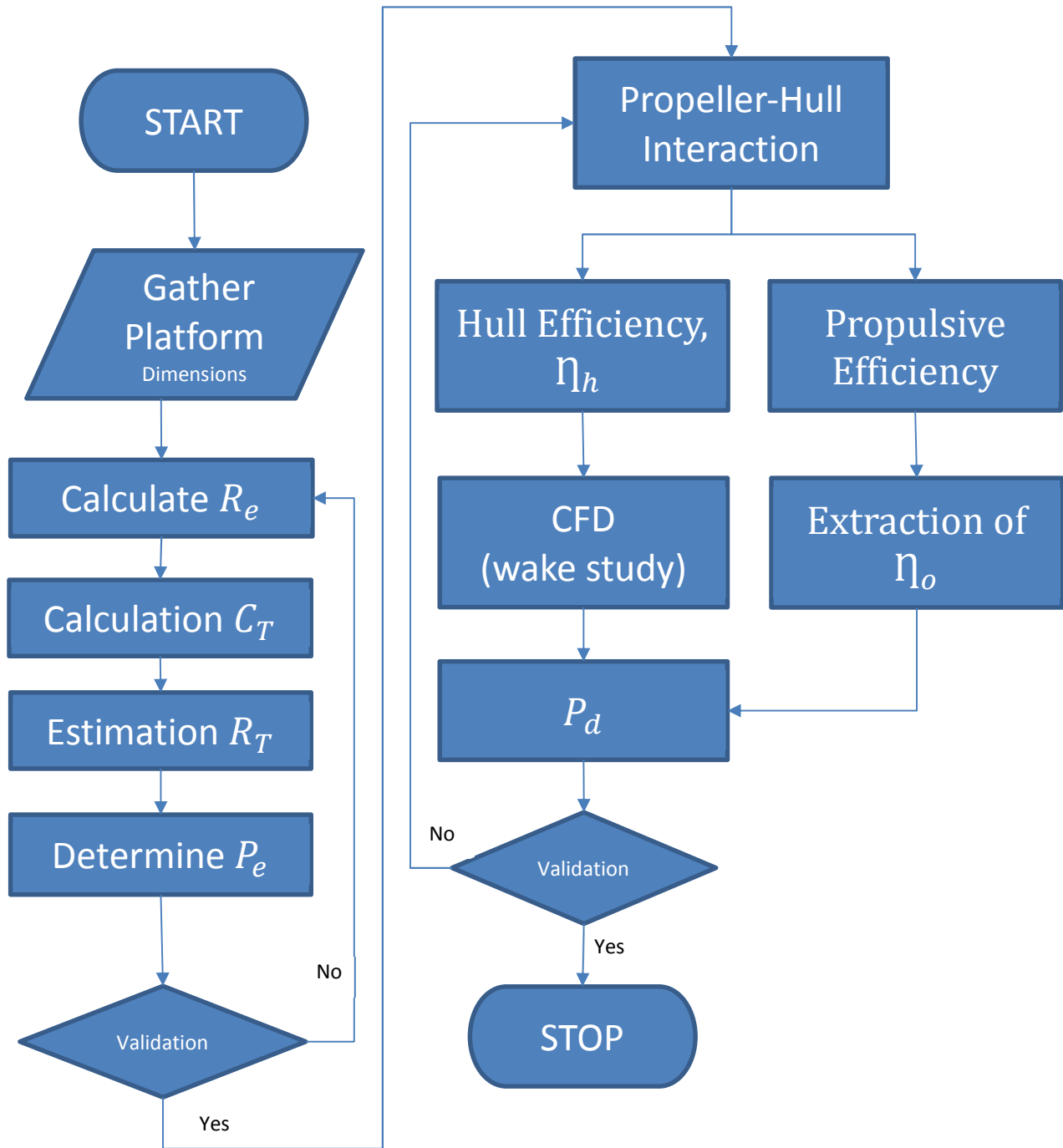Methodology applied in this research follows the flowchart labeled as

Figure 8: Flow Chart for Methodology

Reynolds number is an important parameter to be determined in hydrodynamic analysis as it establish the flow regime in which platform must operate as shown in figure 9 below.
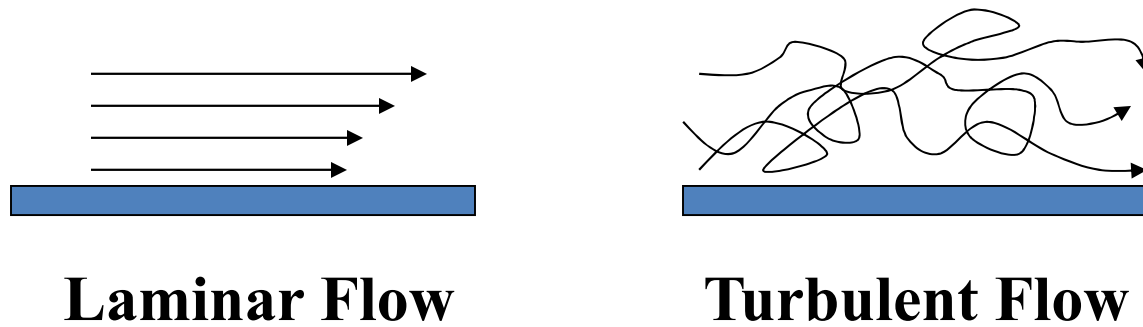

Figure 9: Laminar and Turbulent Flow Patterns

So first, dimensional data of DARPA Suboff was used to calculate the Reynolds Number using equation 1.

$$Re = \partial VL/\mu \qquad \text{Equation 1}$$

Where ∂, is density in Kg/m^3

V, Velocity in m/sec

L, Length overall of DARPA in meters

μ, Dynamic Viscosity (0.001 Pa-s)

Once turbulence of the fluid flowing around the platform has been established, then coefficients of drag will be calculated. Skin friction drag is a function of Reynolds number as increase in Reynolds number will reduce the boundary layer thickness. [39]

Total Drag (C_T) = Frictional Drag (C_f) + Pressure Drag (C_p)   Equation 2

Similarly, equation 2 can be rephrased as $C_T = C_{tangential} + C_{normal}$. Where, coefficient of total drag is an algebraic sum of drag due to tangential force called skin friction drag and drag due to normal force component of water viscosity called as pressure drag.

Whereas, skin friction drag is calculated using ITTC 1957 [40] correction line (close to Hughes flat plate friction) which is equation 3.

$$C_f = \frac{0.075}{(log_{10}Re-2)^2}$$
Equation 3

Since pressure drag is very low, almost 20% of total drag therefore this drag due to pressure difference at bow and stern has been calculated as a function of friction drag using Renilson method [41]

$$Cp = Kp \text{ x } CFform$$
Equation 4

Where,
$$K_p = \xi_{hull} \left(\frac{L}{D}\right)^{-1.7}$$
Equation 5

Value of $\xi_{hull} = 6.0$ for parallel middle body hull-forms

Consequently, total resistance to the motion of platform, measured in Newtons has been calculated using equation 6.

$$R_T = \frac{1}{2}C_d \rho \text{ S } V^2$$
Equation 6

Where, S is the wetted surface area of DARPA Suboff and V is the velocity at which platform is moving in a straight line

Effective Power is the power required to tow a platform without propeller behind it, in a straight line at prescribed velocity in calm waters. Power increases exponentially with increase in velocity of platform.

$$P_E = R_T V$$
Equation 7

The results drawn empirically have been validated. If the results don't match process would have to start from the beginning i.e. calculation of Reynolds Number.

We had a glimpse of resistance force and power required to overcome this resistance force, to tow a platform without propeller. Hereafter, behavior of hull when attached to propeller will be analyzed. The most important parameters to consider in a hull-propeller interaction are:

- Wake Coefficient

- Thrust Deduction Coefficient

- Propulsive Efficiency

Wake is an uneven flow pattern developed at the aft of platform due to the shape of cone, (as the shorter tail cone angle with more length will increase the skin friction drag and higher cone angle with shorter length can cause flow separation) as the velocity decrease at cone of the platform in the position of propeller plane. Moreover, the skin friction due to presence of boundary layer and slow motion of this boundary layer augments the effects cause by slowing of velocity at cone.

There are two types of wake in terms of its measurement i.e. wake measured with propeller present is called *effective wake* and wake measured without propeller plane is called *nominal wake.*

Propellers produce thrust as the water accelerate through it, this phenomenon decreases pressure and increases flow velocity just before entering the propeller, as shown in figure 10.

It is noteworthy that this increase in resistance due to propeller action is called as thrust deduction
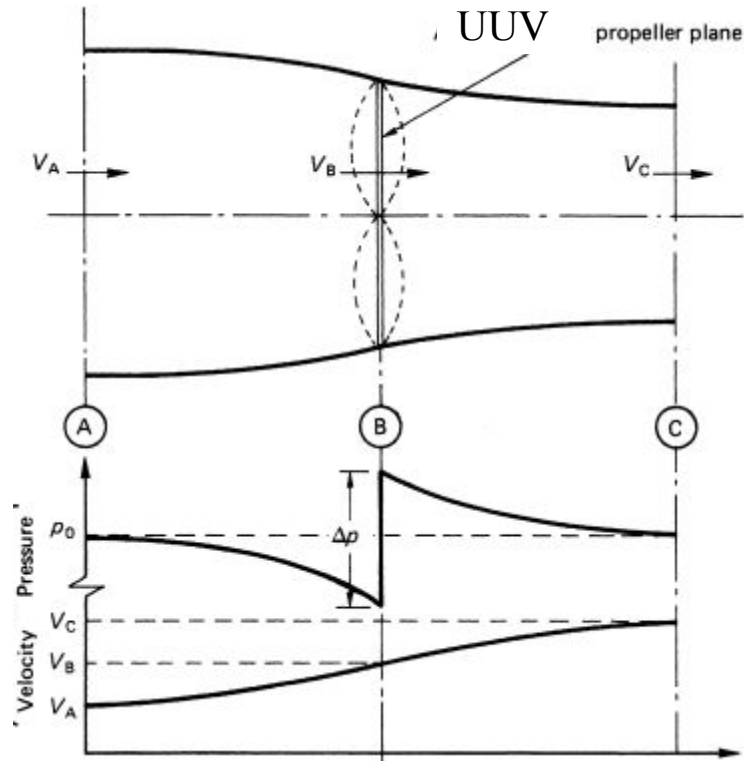
Figure 10: Thrust Deduction

Propulsive efficiency mainly depends on propeller open water behaviors. i.e. efficiency of propeller while operating without ship Infront of it. Moreover, the ratio of torque required by a propeller during cavitation tunnel testing to torque required when operating behind a ship is called as relative rotative efficiency (RRE).

The moments and forces due to pressure/ velocity variation, produced by the propeller are expressed in terms of non-dimensional characteristics for a specific geometric configuration in a Propeller open water diagram (POWD). POWD of an INSEAN E-1619 and DTMB-4119 propellers is shown below.
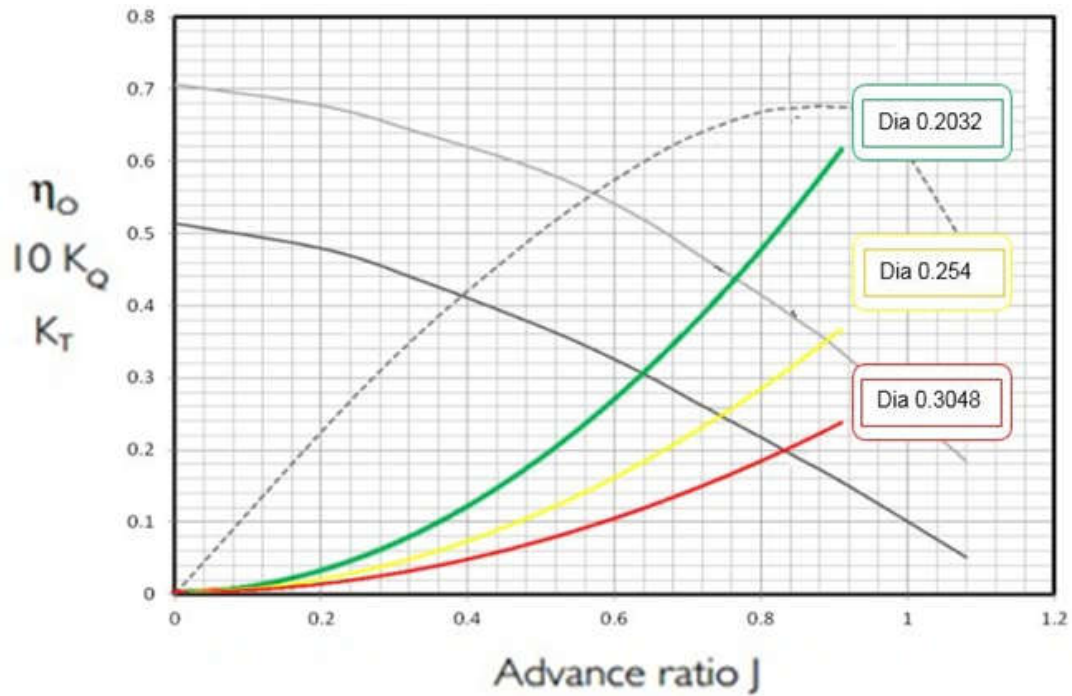
Figure 11: POWD INSEAN E-1619

Where, **Thrust Coefficient,** $K_T = \dfrac{T}{\rho n^2 D^4}$

Torque Coefficient, $K_Q = \dfrac{Q}{\rho n^2 D^5}$

Advance Coefficient, $J = \dfrac{V_a}{nD}$

T = Thrust (N)

Q = Torque (N-m)

Va = Advance/ Average Velocity at propeller plane (m/sec)

n = Revolutions per minute (RPM)

D = Propeller Diameter

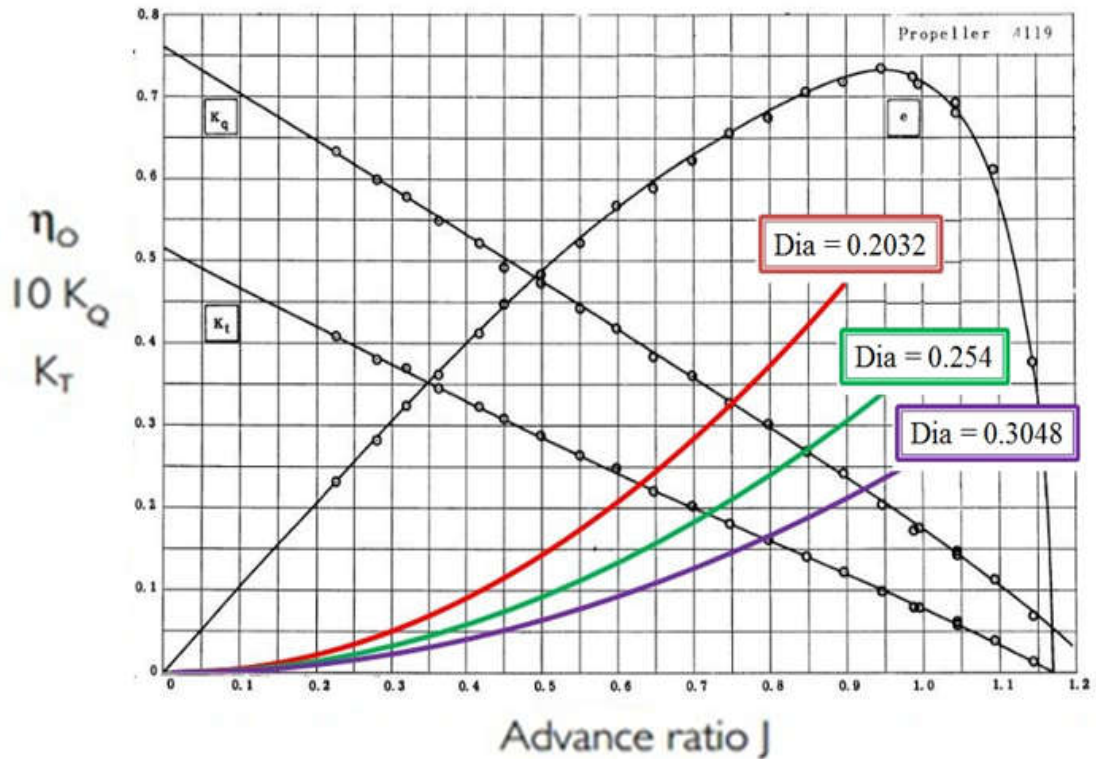ρ = Density of water (1025 kg/m^3)

Figure 12: POWD DTMB-4119 Propeller

Study of these Diagrams reveal that propeller with comparatively large diameter and a smaller number of blades are more efficient, whereas propeller with small diameter are less efficient with less number of blades and become slightly more efficient when number of blades for smaller diameter propellers are increased.

In order to perform the numerical analysis for wake study at aft and to determine the average velocity at tail region of DARPA Suboff, COMSOL Multiphysics was used. Literature survey also endorsed the usage of COMSOL, as currently buoyancy engine UUV's [20] are being numerically analyzed in COMSOL Multiphysics 5.6.

COMSOL Multiphysics is multidimensional solver and analysis tool that can handle phenomenon's involving Multiphysics. It has the capability to solve the system of complex coupled partial differential equation (PDA). COMSOL provides a smooth workflow for computational fluid dynamics problems.

34

Since we must investigate the hydrodynamics of DARPA Suboff at 18 Knots therefore choice of Turbulence model in software requires the basic knowledge of turbulence tools being offered.

Different turbulence models available in the COMSOL Multiphysics proposes multiple formulations for solving problems directly related to turbulent flow like L-VEL or algebraic yPlus. You can also choose among k-ε, Spalart-Allmaras, SST, k-ω, v2-f turbulence models and low Reynolds number k-ε.

Introduction to Turbulence Modeling in COMSOL [42]

In a flat plate fluid flow, as the uniform velocity profile enters flat plate, a laminar boundary layer begins to develop. As the fluid travels some distance away from the leading edge of flat plate, small chaotic oscillations begin to develop in the boundary layer and the flow begins its transition to turbulence, thus becoming fully turbulent flow as shown in fig 13 below.
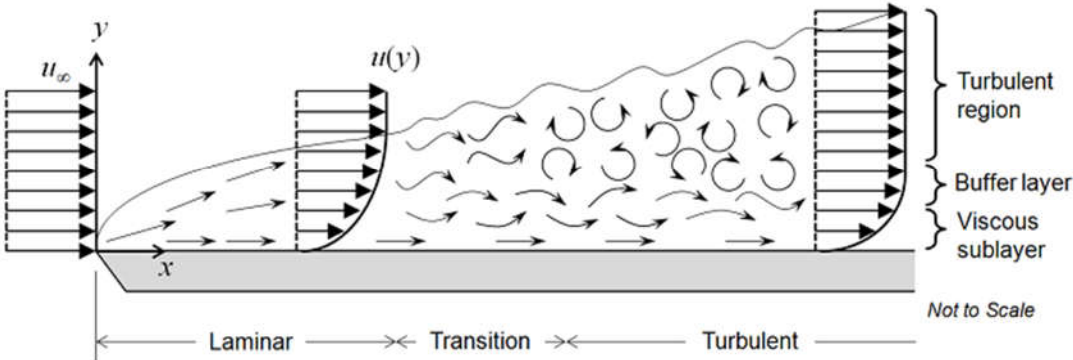

Figure 13: Flow Over a Flat Plate

As with water, viscous stress is proportional to dynamic viscosity as a proportionality constant, as well as shear rate. Although density varies with pressure, it is assumed here that the fluid is marginally compressible, implying that the Mach number is less than 0.3.

In COMSOL Multiphysics, the weakly compressible flow option for fluid flow interfaces ignores the influence of pressure waves on the flow and pressure fields.

The fluid flow in the stratified regime will be governed by the Navier-Stokes equations, which provide the rate and pressure fields. The flow field exhibits tiny eddies as the Reynolds variety grows, and the spatial and temporal scales of the oscillations become so small that they're computationally impossible to resolve using the Navier-Stokes equations, at least for many realistic scenarios.

We can apply a Reynolds-averaged Navier-Stokes (RANS) formulation during this flow regime, which is based on the observation that the flow field (u) over time contains small, native oscillations (u') and can be addressed in a very time-averaged sense (U).

Extra transport equations for turbulence variables, such as the turbulence mechanical energy (k in k-epsilon and k-omega), are provided for one- and two-equation models. To explain the turbulence intensity in pure mathematics models, algebraic equations relying on the rate field and, in some situations, the gap from the walls are introduced.

An eddy consistence that adds to the fluid's molecular viscosity is determined using the turbulence variable estimates. The momentum that the small eddies will transfer is instead converted to a viscous transport.

Apart from the viscous sublayer on the edge of solid walls, turbulence dissipation normally takes precedence over viscous dissipation everywhere. As with low Reynolds variety models, the turbulence model should constantly reduce the turbulence level. Alternatively, new boundary conditions must be determined using wall functions.

Physics in the near Wall Region:

Four regions of turbulence near a boundary wall are appended below:

1. When the average flow velocity is proportional to the log of the distance to the wall, the flow connects to a region where it becomes a completely turbulent flow. This is referred to as the log-law region.

2. The buffer layer is a region located further away from the wall. Turbulence stresses begin to take precedence over viscous stresses in the buffer region.

3. The fluid velocity is zero at the wall, and the flow velocity is linear with distance from the wall in a thin layer above it. This is known as the viscous sublayer or laminar sublayer.

4. The flow transitions to the free-stream region as it moves further away from the wall.

A RANS model can be used to compute the flow field in all four of these regions. However, because the buffer layer's thickness is so small, it may be advantageous to use an approximation in this region.

Wall functions disregard the flow field in the buffer zone and compute an analytical nonzero fluid velocity at the wall. When you employ a wall function formulation, you assume an analytic solution for the flow in the viscous layer, which results in substantially lower processing needs for the resultant models. This is a very handy method for a broad variety of real engineering applications.

If more accuracy is desired than what the wall function formulations provides, a turbulence model that solves the entire flow regime can be considered as an additional help, as described above for the low Reynolds number models. Computation of lift and drag on an object, or the heat transfer between the fluid and the wall can be analyzed using these configurations.

COMSOL employs eight alternative Reynolds Averaged Navier Stoke turbulence models, which differ in how they handle flow near barriers, the quantity of extra variables solved for, and the meaning of these variables. All these models add an extra turbulent eddy viscosity element to the Navier-Stokes equations, although they do it in different ways.

The **Spalart-Allmaras** model adds a single variable to account for undamped kinematic eddy viscosity. It is a low Reynolds number model capable of resolving the whole flow field all the way down to the solid wall.

The model was initially designed for aerodynamics applications and has the benefit of being reasonably durable with low resolution requirements. This model does not properly compute fields with shear flow, separated flow, or fading turbulence, according to experience. It has the virtue of being fairly stable and exhibiting good convergence.

The eddy viscosity is computed by the algebraic **y+Plus and L-VEL** turbulence models listing algebraic formulas based solely on the local fluid velocity and distance to the nearest wall. They don't solve any other system of equations.

These models, which are the most durable and least computationally costly of the eight turbulence models, solve for flow everywhere. While they are often the least accurate models, they do give reasonable internal flow estimates, particularly in electronic cooling applications.

The **k-omega (k-ω) model** is like the k-epsilon model, except it solves for (omega) which is the rate of kinetic energy dissipation. It is a low Reynolds number model that may also be utilized with wall functions. It is more nonlinear and hence more difficult to converge than the k-model, and it is very sensitive to the initial guess of the solution.

In many circumstances when the k-epsilon model is inaccurate, such as internal flows, flows with severe curvature, divided flows, and jets, the **k-omega model** is beneficial. Flow through a pipe bend is a nice illustration of internal flow.

The **k-epsilon model** solves for two variables: k, the turbulence kinetic energy, and epsilon, the rate of turbulence kinetic energy dissipation. Because this model employs wall functions, the flow in the buffer zone is not simulated.

k-epsilon model has a high convergence rate and minimal memory needs. It does not compute flow fields with unfavorable pressure gradients, high flow curvature, or jet flow very correctly. It works effectively for exterior flow issues involving complicated geometry.

The **low-Reynolds-number k-epsilon model** is similar to the k -ε model, however, it does not need the use of wall functions: it can solve for flow everywhere. It is a logical extension of the k-model and shares many of its advantages, but it usually necessitates a denser mesh; not only at walls, but anytime its low Reynolds number features kick in and reduce the turbulence.

It is occasionally advantageous to utilize the k-ε model to first obtain an appropriate starting condition before solving the **low Reynolds number k-epsilon model**.

Another option is to employ the automated wall treatment, which begins with a coarse boundary layer mesh to obtain wall functions and then refines the boundary layer at the interesting walls to provide low Reynolds number models.

Close to the boundary of a wall, the changes of velocity are frequently significantly bigger in parallel directions to the wall than in perpendicular directions to the wall. The velocity variations are considered to be anisotropic. Further away from the wall, the oscillations are of same amplitude in all directions. The velocity variations become isotropic.

In addition to the two equations for turbulence kinetic energy (k) and dissipation rate (ε), the **v2-f turbulence model** describes the anisotropy of turbulence intensity in the turbulent boundary layer using two additional equations.

The first equation addresses the transfer of turbulent velocity fluctuations normal to the streamlines. The second equation compensates for non local phenomena such as wall-induced dampening of the redistribution of turbulence kinetic energy between normal and parallel directions.

The **SST model** is a hybrid of the k-ε model in free flow and the k-ω model near the walls. It is a low Reynolds number model that is commonly used in industrial applications. It has comparable resolution requirements to the k-ω model and the low Reynolds number k-epsilon model, but its formulation overcomes some of the shortcomings of the pure k-ω and k-epsilon models.

The wall resolution viscous units must be confirmed during wall function formulation (this plot is generated by default). This number indicates how far into the boundary layer computational domain the computation begins, and it should not be too big.

If the wall resolution surpasses a few hundred, consider refining the mesh in the wall normal direction. The second variable to consider when employing wall functions is the wall liftoff (in length units). This variable is connected to the estimated thickness of the viscous layer and should be tiny in relation to the geometry's surrounding dimensions. If it isn't, then refine the mesh in these areas as well.

CAD file of DARPA was created with available dimensions and published offset data [36] and same was imported in .stp format in COMSOL. The process adapted in CFD study is explained in flowchart as figure 14 below
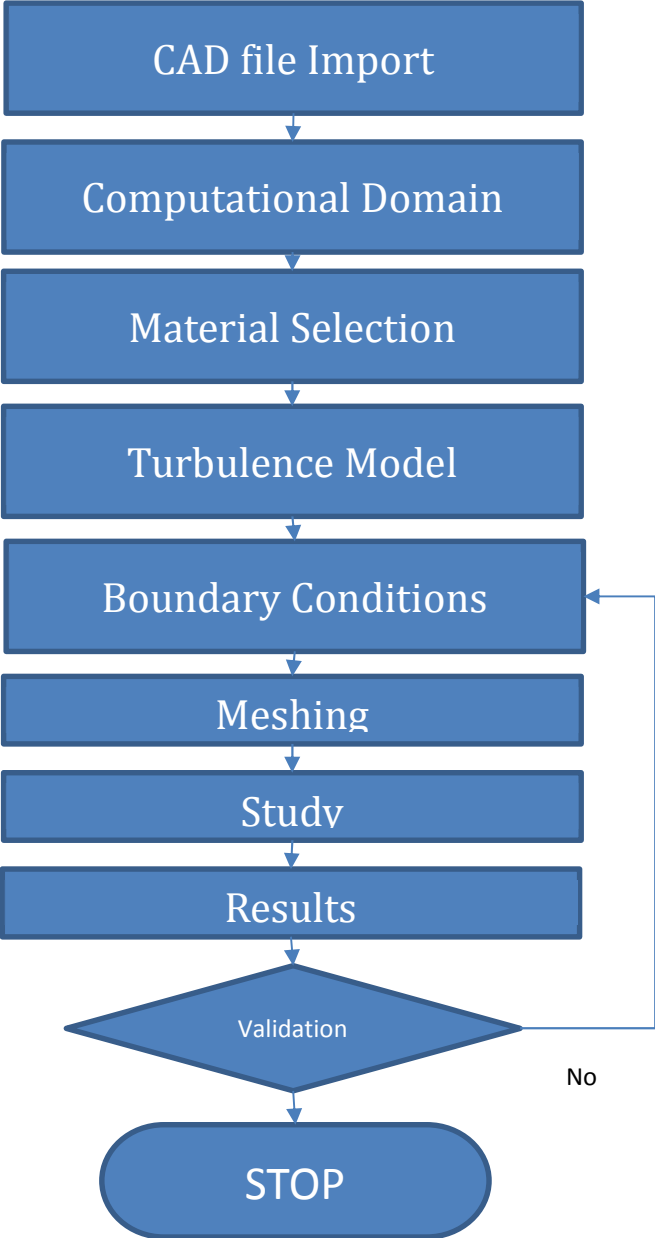
Figure 14: Flow Chart for CFD in COMSOL

After importing the model, computational domain, (fig 9) was defined in accordance with ITTC [38] guidelines for RANS calculations of Nominal Wakes.
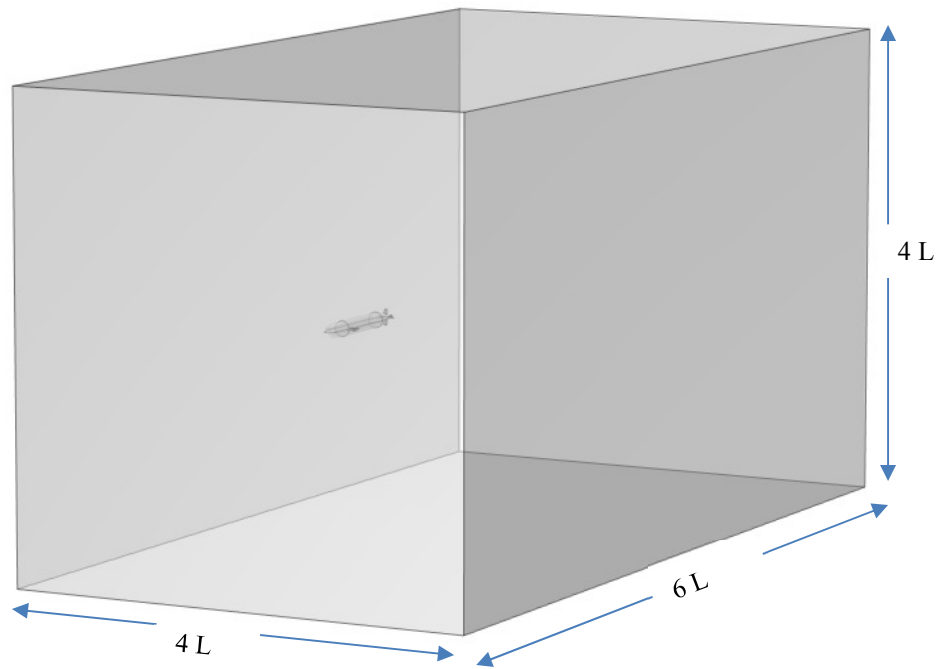

Figure 15: Computational Domain

Length, breadth and height of this computational domain were set as 6L, 4L and 4L respectively. Where L is the overall length of platform mentioned earlier. Platform was placed in middle of block to avoid the wall effects and to simulate a towing tank.

DARPA platform was subtracted from computational domain using Boolean operation tool. Water was defined as material around DARPA hull form.

Since we are interested to compute the flow behavior around DARPA Suboff therefore turbulence model with external flow estimation feature has been the priority. So, as discussed above K-epsilon turbulence model with wall function has been selected, as it has the ability to analyze the Turbulent

regime with no slip conditions at wall and also most of the published data has used k-epsilon solver to solve Reynolds Averaged Navier Stoke Equations (RANS).

RANS Method

RANS method uses the continuity equation and equations for the unsteady, three-dimensional and incompressible flow as the leading equations. These equations are the continuity equation as shown below

$$\frac{\partial U_i}{\partial x_i} = 0$$

Whereas momentum equation is as follow:

$$\frac{\partial U}{\partial t} + \frac{\partial \left(U_i U_j \right)}{\partial x_j} = -\frac{1}{\rho}\frac{\partial P}{\partial x_i} + \frac{\partial}{\partial x_j}\left[\nu \left(\frac{\partial U_i}{\partial x_j} + \frac{\partial U_j}{\partial x_i} \right) \right] - \frac{\overline{\partial u_i' u_j'}}{\partial x_j}$$

For steady state case, the first term in above equation is not considered. In momentum equations, Ui and ui' represent the mean velocity and the fluctuation velocity components in the direction of the Cartesian coordinate *xi*, respectively. P, ρ and ν express the mean pressure, the density and the kinematic viscosity coefficient, respectively.

Additional equations known as transport equations and variables are employed by the *k*-ε model i.e. two (2) dependent variables: the turbulent kinetic energy, *k*, and the turbulent dissipation rate, ε. The turbulent viscosity is modeled as

$$\mu_T = \rho C_\mu \frac{k^2}{\varepsilon}$$

Where, model constant is denoted as C_μ.
The transport equation for *k* reads:

$$\rho\frac{\partial k}{\partial t} + \rho\mathbf{u}\cdot\nabla k = \nabla\cdot\left(\left(\mu + \frac{\mu_T}{\sigma_k} \right)\nabla k \right) + P_k - \rho\varepsilon$$

where the production term is

$$P_k = \mu_T\left(\nabla\mathbf{u}:(\nabla\mathbf{u} + (\nabla\mathbf{u})^T) - \frac{2}{3}(\nabla\cdot\mathbf{u})^2 \right) - \frac{2}{3}\rho k\nabla\cdot\mathbf{u}$$

The transport equation for ε reads:

$$\rho \frac{\partial \varepsilon}{\partial t} + \rho \mathbf{u} \cdot \nabla \varepsilon = \nabla \cdot \left(\left(\mu + \frac{\mu_T}{\sigma_\varepsilon} \right) \nabla \varepsilon \right) + C_{\varepsilon 1} \frac{\varepsilon}{k} P_k - C_{\varepsilon 2} \rho \frac{\varepsilon^2}{k}$$

The model constants in above equations are determined from experimental data [43] and the values are $C_u = 0.09$, $C_{\varepsilon 1} = 1.44$, $C_{\varepsilon 2} = 1.92$, $\sigma_k = 1.0$ and $\sigma_\varepsilon = 1.3$ respectively

The Model Limitations for k-ε turbulence model relies on an assumption that the flow around subject of study is at very high Reynolds number. This consequently implies that the turbulence has achieved an equilibrium in boundary layers i.e. which means that production equals dissipation.

Such prospects limit the efficacy of this turbulence model because these assumptions are not always true. Specifically, it does not respond correctly to flows with adverse pressure gradients and can result in under-prediction of the spatial extent of recirculation zones. Furthermore, in simulations of rotating flows, the model often shows poor agreement with experimental data.

Discretization of Fluids [44]

Most physics interfaces in COMSOL Multiphysics use the finite element method to solve the underlying partial differential equations. The finite element method separates the modelling domains into smaller, simpler domains called elements. The solution is reached by constructing and solving a set of equations that span all of the model's components. The solution to these equations is nearly identical to the right solution to the partial differential equation.

The equations within each element are sometimes referred to as form functions and can be in any sequence. In the simplest instance, the shape functions within each element of a one-dimensional finite element model are essentially a collection of polynomials specified over the domain. The set of linear (first-order), quadratic (second order), and cubic (third order) shape functions is displayed in the graphic below. A linear sum of these shape functions is used to solve the problem inside the elements.

•

In many situations, the default discretization is second order (quadratic), which is due in part to the fact that many partial differential equations contain a dominating second derivative component. Fluid flow and transport problems are typically discretized using a first-order, linear discretization. Changing the discretization may be justified depending on the modelling circumstances, and it is feasible to modify the discretization for each separate physical interface independently, although doing so has various ramifications.

Reduced fragmentation without increasing the number of pieces results in a model that takes less computer resources but has worse accuracy. Increasing the discretization without increasing the number of components produces a more accurate answer but necessitates more computer resources.

For quadratic and greater discretization, there are occasionally extra alternatives such as Lagrange and serendipity elements. This option has an effect only if the mesh contains rectangular, prismatic, pyramidal, or hexahedral components.

The Lagrange element adds more nodes (degrees of freedom) to the elements. Although the serendipity element has fewer nodes per element, it frequently offers better accuracy for the same mesh but a lower computational cost than the Lagrange element.

If a mesh dominated by rectangular, prismatic, pyramidal, or hexahedral components can be produced, it is typically worthwhile to use the serendipity discretization, if it is accessible within the physics.

A P1+P1 discretization is the default discretization for laminar and turbulent flow issues. Both the fluid velocity and pressure fields are solved using linear shape functions. It is possible to increase the discretization to P2+P1, showing that quadratic shape functions are employed for velocity but linear basis functions for pressure.

A **P1+P1** discretization is the default discretization for laminar and turbulent flow issues. Both the fluid velocity and pressure fields are solved using linear shape functions.

It is possible to increase the discretization to P2+P1, showing that quadratic shape functions are employed for velocity but linear basis functions for pressure.

In COMSOL Multiphysics, it is the default component request for the Laminar Flow and Turbulent Flow single-progressively ease stream interfaces and the discretization of liquids in the multiphase stream interfaces.

P2+P1 This uses a second-request components for the speed parts and straight components for the tension field. Second-request components function admirably for low stream speeds. This is
•the default component request for the Creeping Flow interface.

P3+P2 implies third-request components for the speed parts and second-request components for the strain field. This can add extra exactness, yet it likewise adds extra levels of opportunity
•contrasted with P2+P1 components.

Boundary Conditions

Boundary conditions were applied as per table 3

Boundary	Conditions
Inlet	Constant Velocity
Outlet	Constant Static Pressure
DARPA Hull	No- Slip Wall
Top	Symmetry
Bottom	Symmetry
Sides	Symmetry

Table 3: Boundary Conditions

Before starting the wake study, a mesh convergence study was done to validate the results. 04 x different mesh types were shortlisted as shown in fig 16 below. It is evident from table 3 that computational time increase with increase in number of elements.

However, the difference in results with fine and finer mesh is in range of up to 5 %. Therefore, Fine mesh was used in rest of the study.

Mesh Type	No. of Elements	Computational Time	R_T (N) Experimental [36]	R_T (N) CFD	% Error
Coarse	348594	44 mins		113.99	14.3
Normal	870091	1 hour 50 mins	102.3	111.60	9.1
Fine	1591069	3 hr 32 mins		108.13	5.7
Finer	7499446	5 hr 27 mins		105.57	3.2

Table 4: Mesh Selection Study
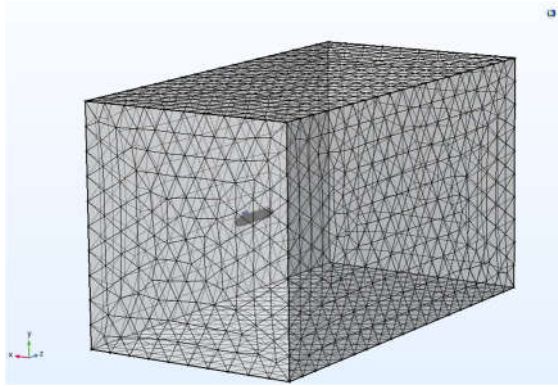
Coarse Mesh
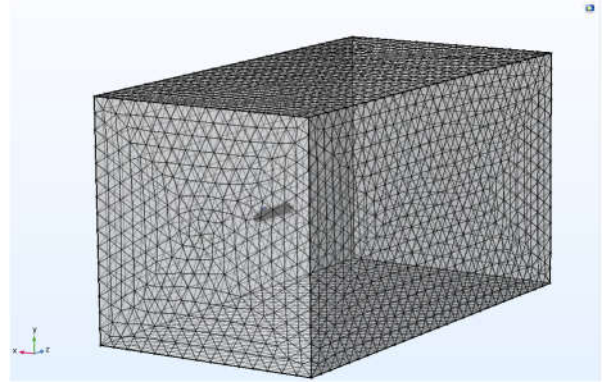
Normal Mesh
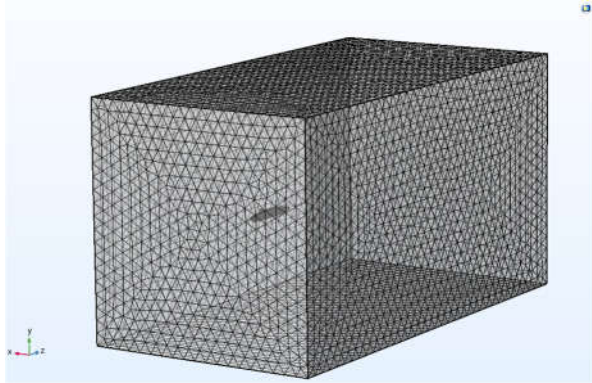
Fine Mesh
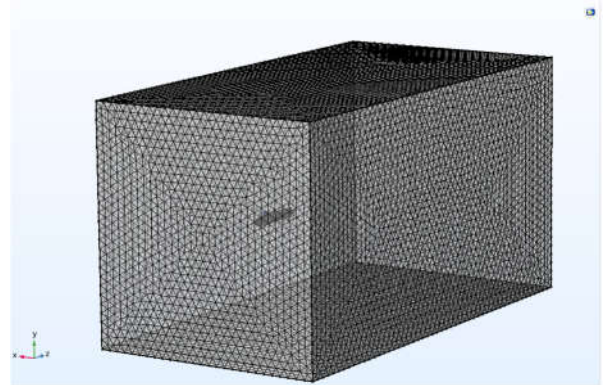
Finer Mesh

Figure 16: Mesh Selection Study

It is worth mentioning that boundary conditions were kept same for all 04 cases of mesh study. Lastly the hull efficiency and propulsive efficiencies will be calculated for 07 x different propeller locations as shown in fig 17 below
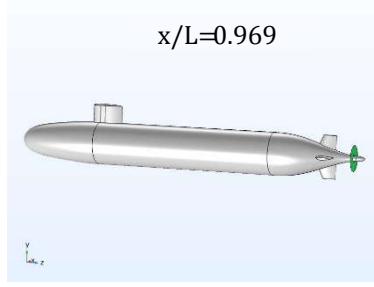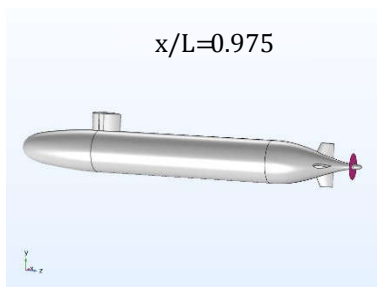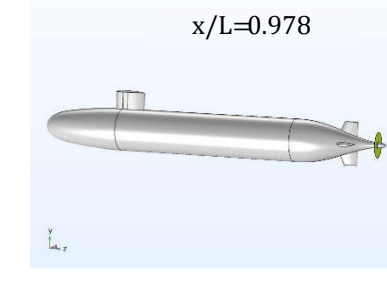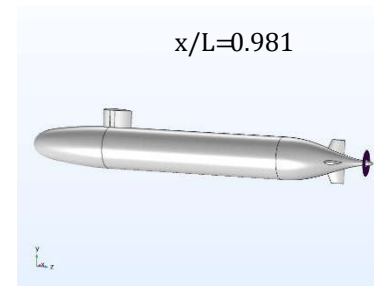
x/L=0.997
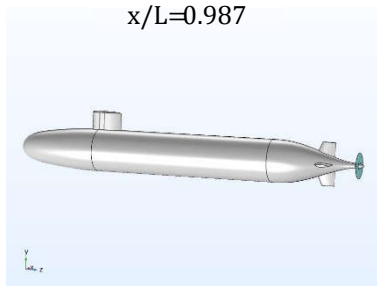
x/L=0.993

x/L=0.987
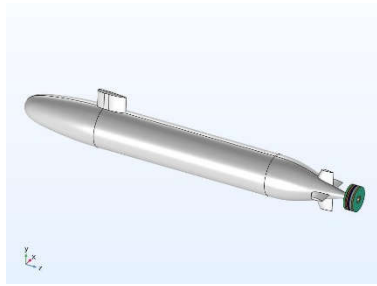
x/L=0.981

x/L=0.978

x/L=0.975

x/L=0.969
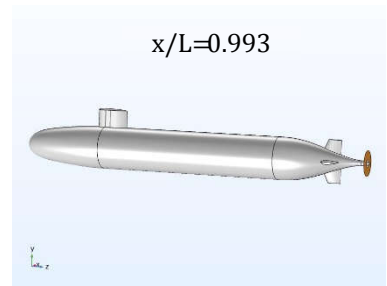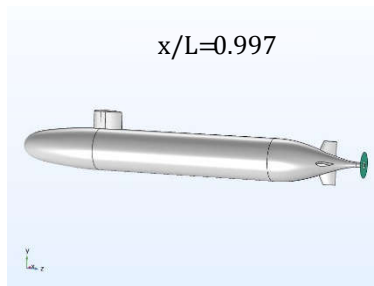
Figure 17: Propeller Plane at 07 x Different Locations

CHAPTER 4 RESULTS

Reynolds number calculated using equation 1 above demonstrates a linear relation between velocity and Reynolds number as shown in figure 18. It is evident that as soon as the platform starts its motions Reynolds number is in its upper limits of laminar flow (Re $\sim 10^6$). This can be better understood when read with boundary layer theory, as soon as the platform starts its motion there is a thick boundary layer attached to the hull as the velocity increases boundary layer thickness decreases consequently, flow becomes turbulent
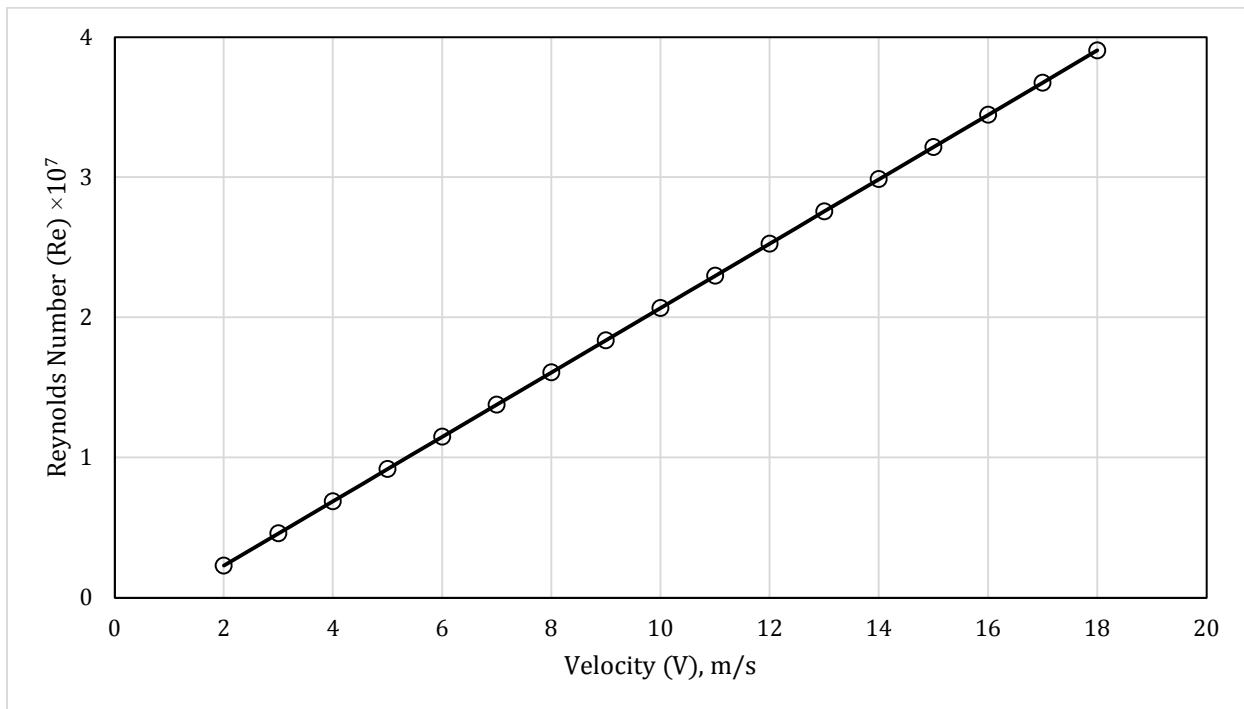

Figure 18: Re vs Velocity Graph

It is worth mentioning that behavior of skin friction drag coefficient and total drag coefficient is a function of Reynolds number (Re) as shown in figure 19 below. As the Re increases, coefficient of skin friction drag decreases, this decline is sharp when Re $< 10^7.$

This phenomenon is due to the fact that upper limit [39] of Laminar flow is 3×10^6. As the flow passes this region smoothing of curves is observed. Moreover, coefficient of skin friction is inversely proportional to Re as explained in equation 3 above.
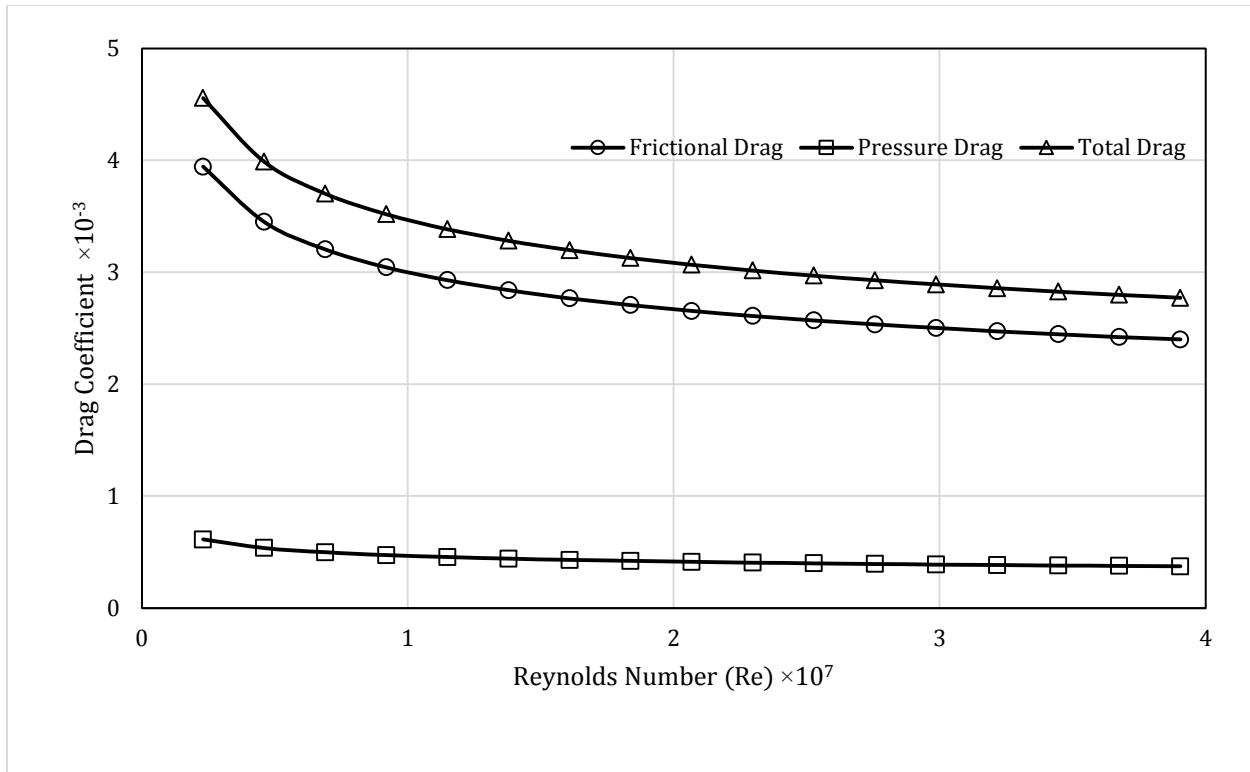
Figure 19: Coefficients of drag vs Re

As the Reynolds number increases flow becomes turbulent therefore, lot of energy is lost in the form of heat dissipation

Total resistance of the platform at different velocities was calculated using equation 6 above, as shown in figure 20 below. It is evident that resistance to the motion of platform increases exponentially with an increase in velocity.
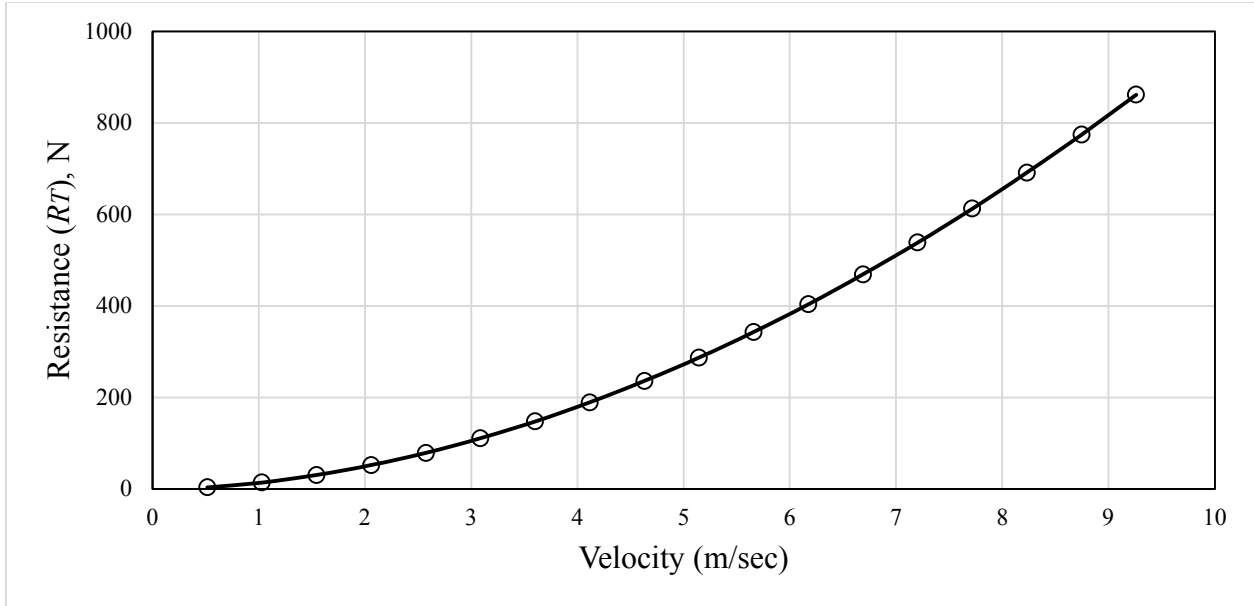
Figure 20: Velocity vs Total Resistance

Additionally, the drag derived from numerical analysis of DARPA Suboff was pitched against published experimental data. It was found that the difference between experimental data and CFD data is less than 4 %. However, the difference between empirically found data and experimental data is approximately 6% as shown in table 05 below

Velocity (m/sec)	R_T(N) Empirical	R_T (N) Experimental [36]	Error (%)
3.051	108.8	102.3	6.4
5.144	287.5	283.8	1.3
6.096	394.6	389.2	1.4
7.161	532.9	526.6	1.2
8.231	691.4	675.6	2.34
9.152	843.2	821.1	2.7

Table 5: Total Resistance

Numerical analysis provides a clear picture of average velocities profile at 07 x different locations with 02 x different propeller diameters. Results are shown in figure 21 below.
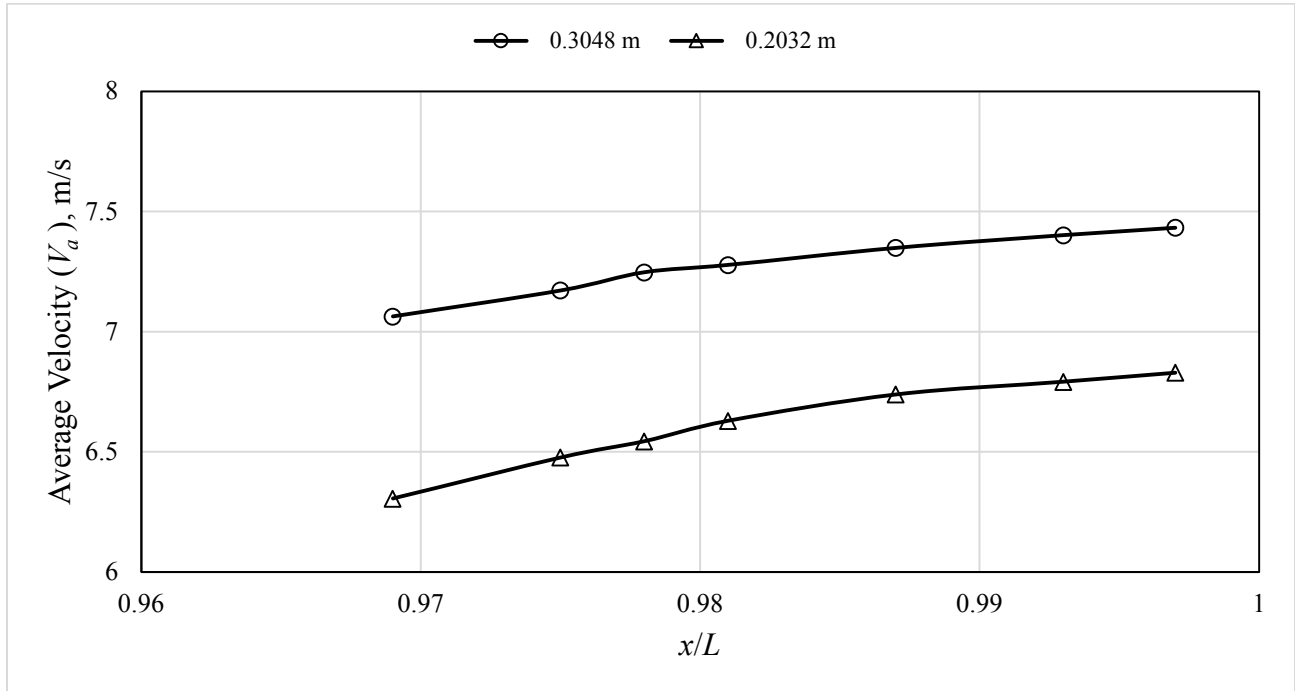

Figure 21: Average Velocity vs Propeller Location

It is evident from graph that average velocity at small diameter propeller is less in comparison to propeller with big diameter. The reason to this problem is that the small diameter of propeller has a better chance to stay in the wake field in comparison to large diameter propeller.

If we keep on increasing the diameter of propeller, a stage will come where propeller blades will be operating outside the slow velocity region known as wake region at the aft of platform, therefore torque requirements for such condition will rise rapidly to provide the platform with same thrust. Propeller efficiency
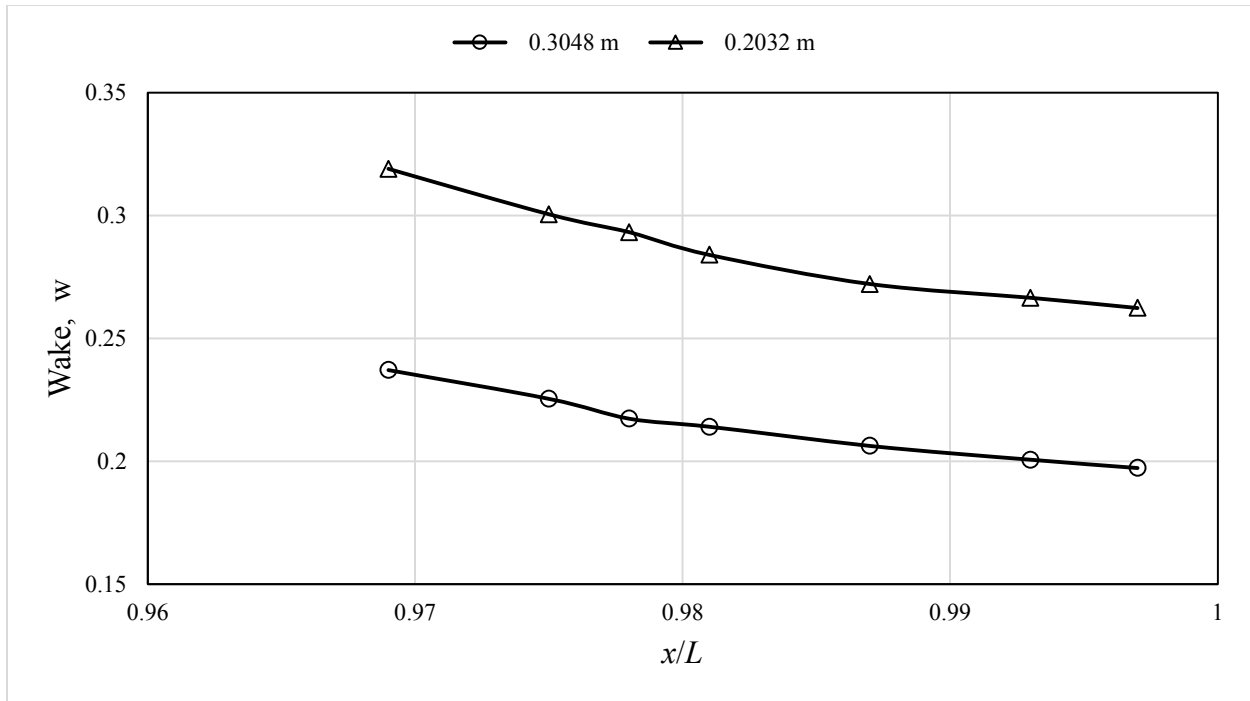
Figure 22: Wake vs Propeller Location

Wake was calculated using Taylor wake fraction (w), as logically predicted wake is more for small propeller diameters as shown in fig 16. Pictorial representation of wake at tail is listed below in fig 23.
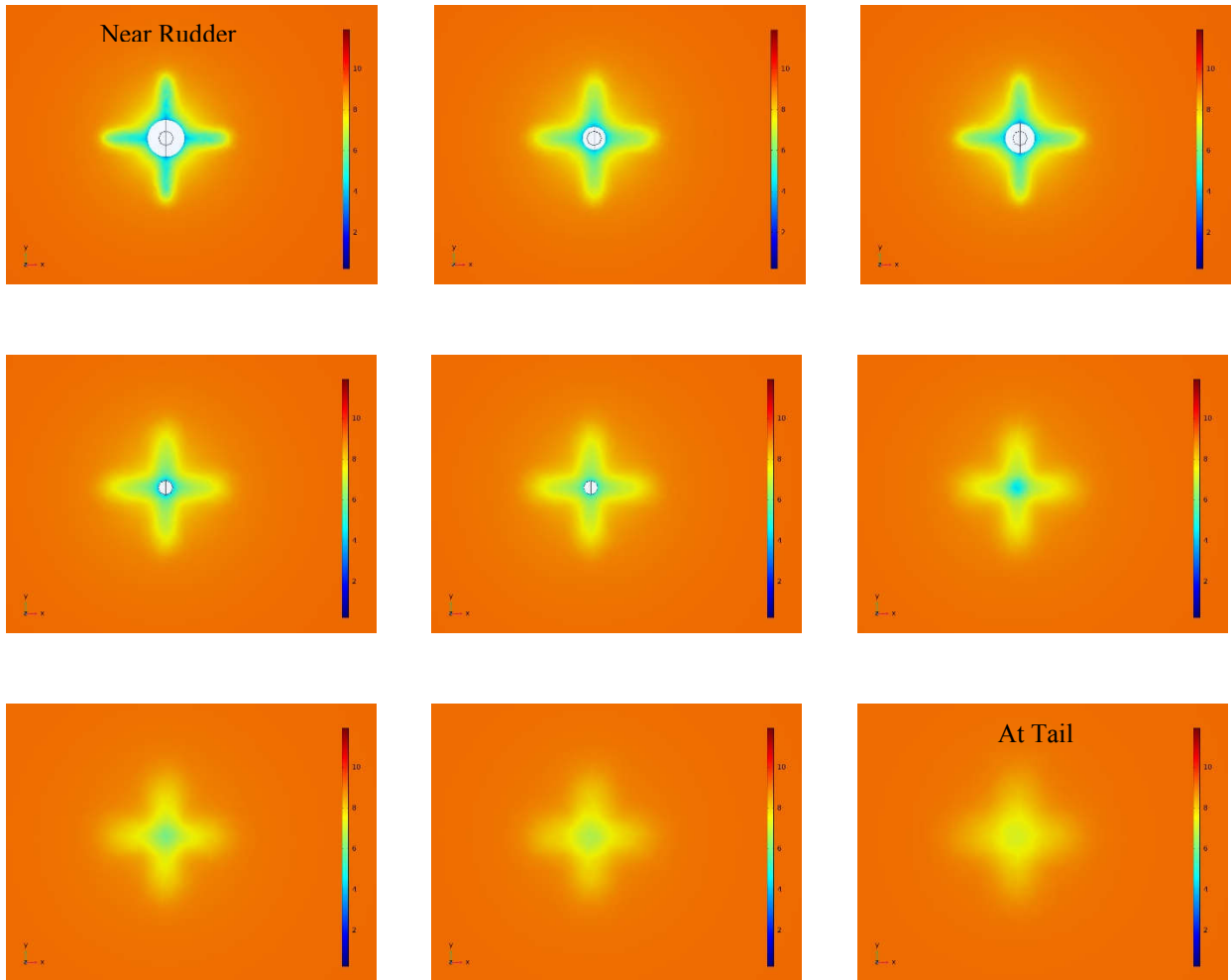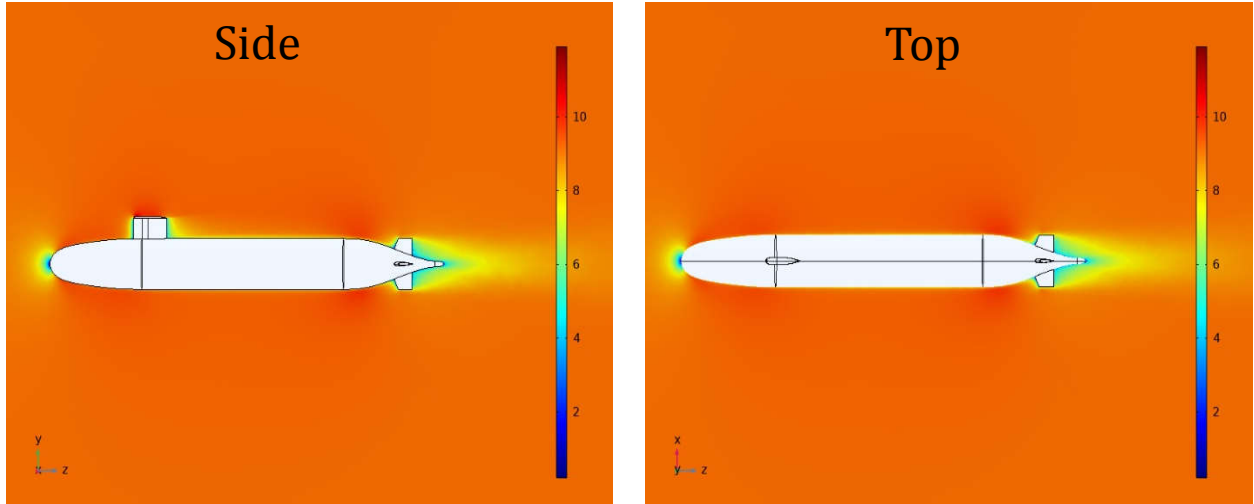
Figure 23: Wake profile at aft

Based on this wake profile, hull efficiency was derived. Hull efficiency is a ratio of Thrust Power and Effective Power. It's not a true efficiency but ratio of efficiencies. Hull efficiency declines as the propeller moves away from rudder.
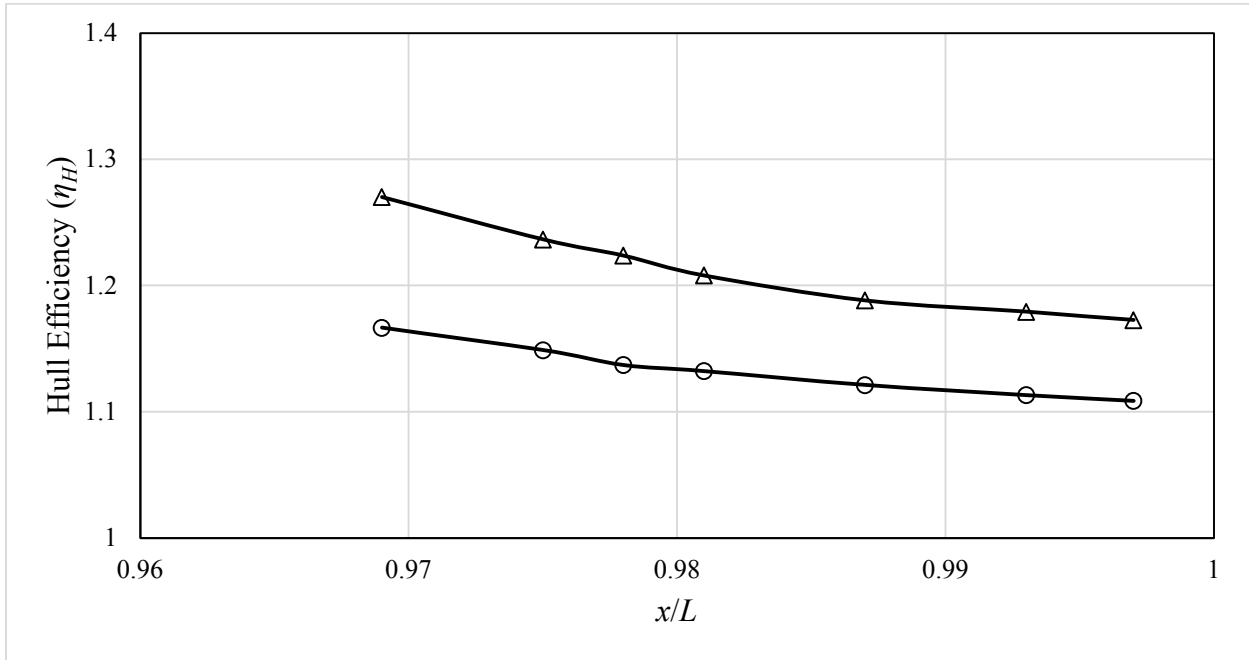

Figure 24: Hull Efficiency vs Propeller Location

Thrust Power is output power i.e. power produced by propeller to generate required thrust. Big propellers will require generate more thrust power as shown in figure 25.
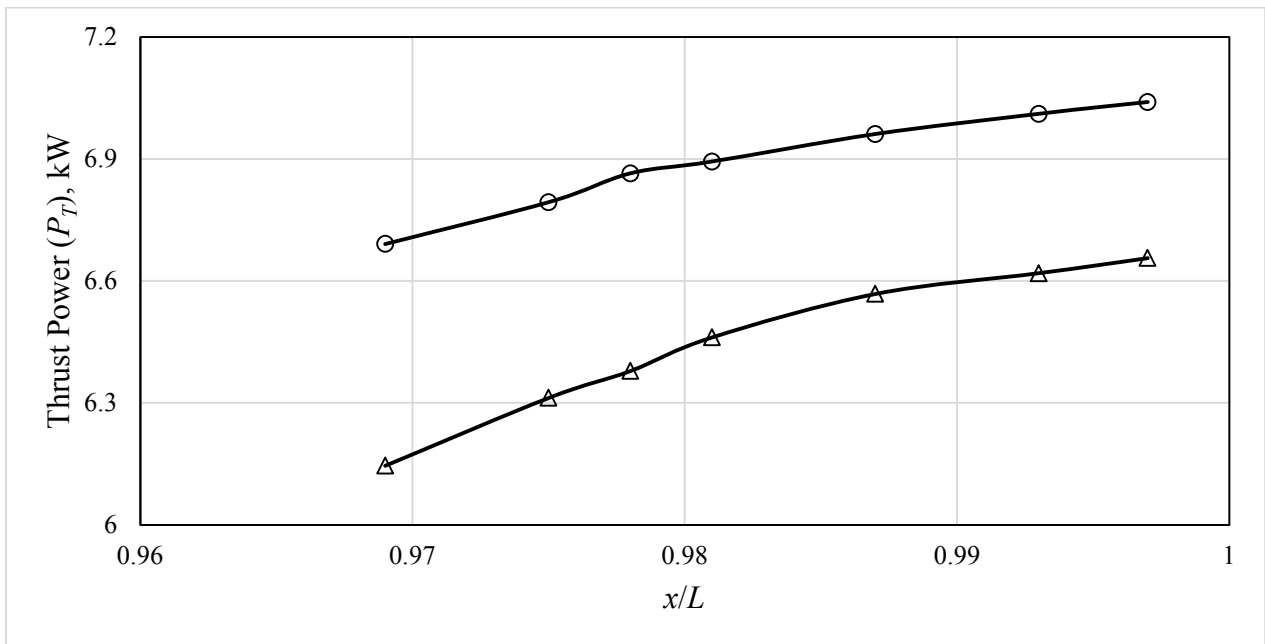

Figure 25: Thrust Power vs 7 Locations

Propeller open water efficiency is an important factor to assess the performance of propulsion chain, since we are using 02 different diameters of propellers, so B-Series [45] propeller open water data was used to asses the open water efficiency of four different propellers as shown in fig 26 below.
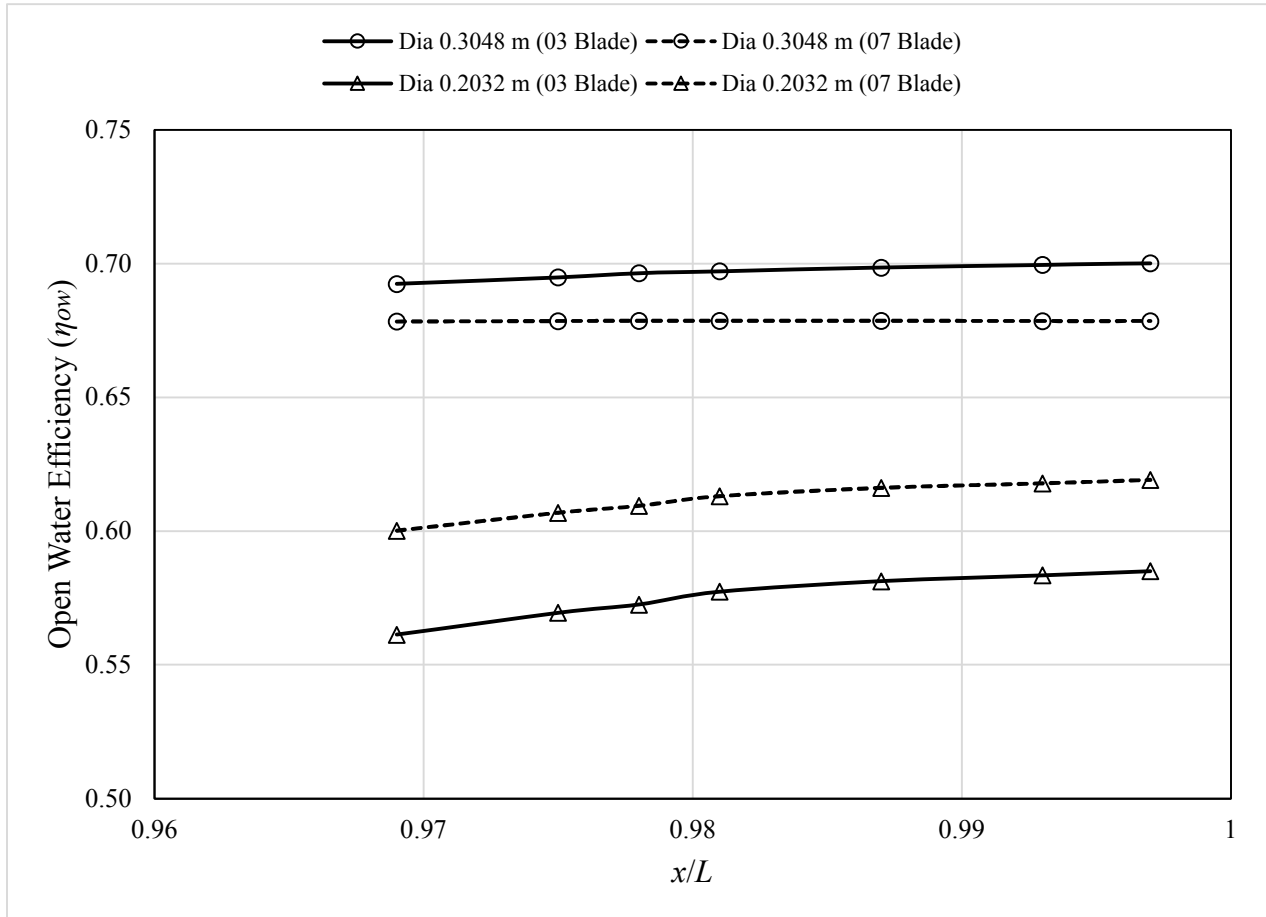
Figure 26: Propeller Open Water Efficiency vs 07 Locations

It is evident that propeller with a smaller number of blades must rotate more to produce the same thrust. Hence Propeller with large diameter and a smaller number of blades is more efficient as compared to the other propellers.

Delivered Power (P_D) is the input power to propeller. i.e. Power delivered to propeller to generate the thrust, Since, we are dealing with propellers with 02 x different diameters and 02 x different

blade configurations, therefore the behavior of 3 blade propeller observed is shown in figure 27 below

Figure 27: 3 Blade Propeller Delivered Power vs 07 Location
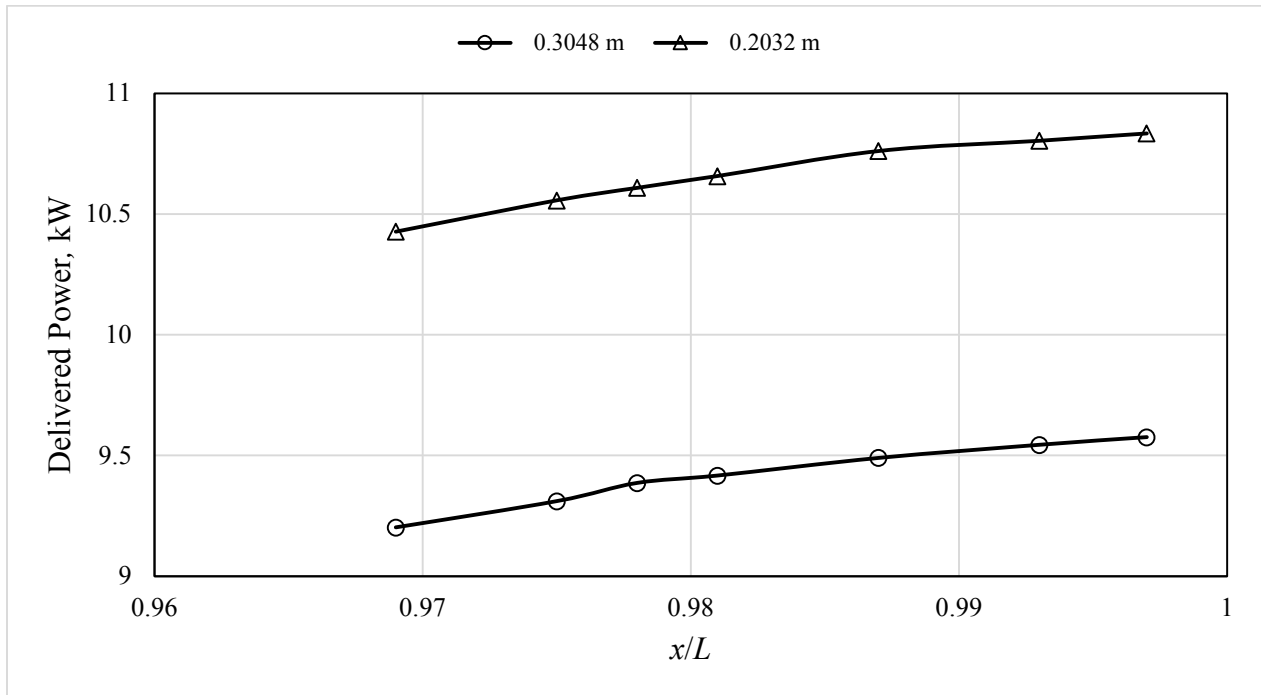
It is evident that the 3 bladed propellers with bigger diameter is much efficient in comparison to the similar propeller with less diameter. However, one important thing to observe is that the input power requirements increases as we move towards the tail of the platform.

When we compare propellers with 07 blade configuration as shown in fig 28 below, similar behavior is observed as in the case of 03 blade propellers. Propellers with big diameters proves to be more efficient.

However, again as we move away from the rudders, the energy required to power the propeller increases. Hence there is a limit to the hydrodynamic gain with a very large diameter propeller
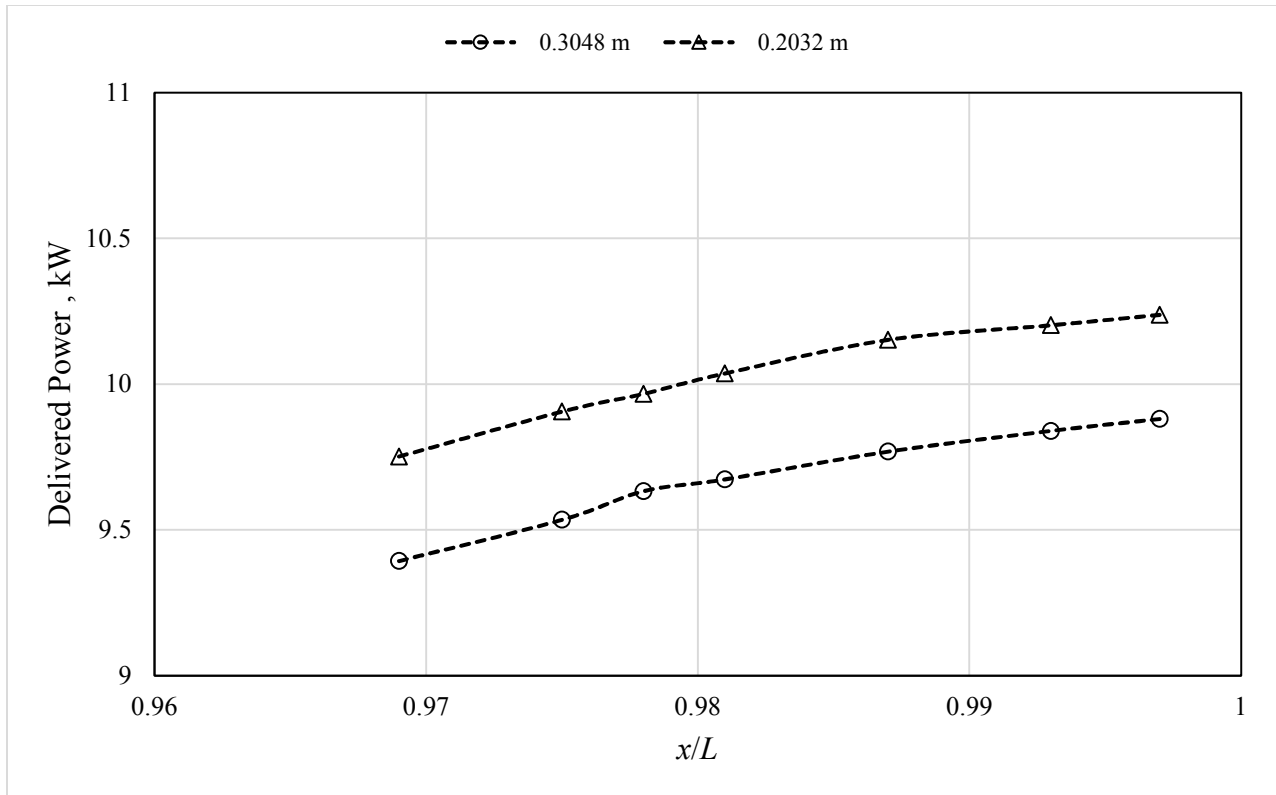
Figure 28: 07 Blade Propeller Delivered Power vs 07 Location

The above trends can also be proved with the help of propulsive efficiency, i.e. the efficiency of complete propulsion system as shown in fig 29 below

Part of overall propulsive efficiency are the mechanical losses incurred in transmitting the power from the propulsion motor along the shaft to the propulsor. These are mainly frictional losses in bearings, seals and possibly gearing if installed. Though usually accounting for only a small loss in efficiency they again need to be considered in the configuration of the stern arrangements.

Figure 29: Propulsive efficiency vs Locations

Propellers with large diameters are more efficient and propulsive efficiency decreases as we move towards the tail of platform.

CHAPTER 5 – CONCLUSION
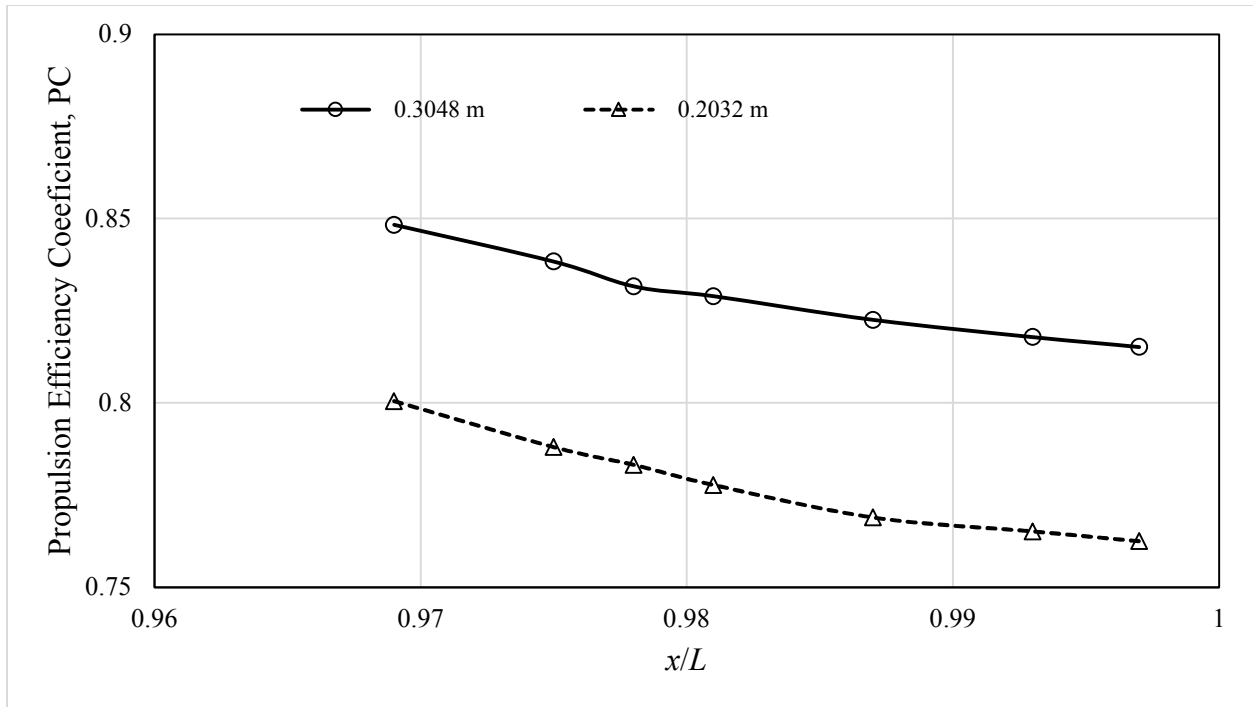
In this research work DARPA Suboff platform resistance is calculated and validated with the available published data. Both Computational fluid dynamics and empirical approaches converge on same results with a slight difference from experimental data. Average velocity at 07 x different propeller planes with 02 x different propeller diameters leads to an important uneven flow patterns at the entry of propulsor This resultant wake study is significant to understand the flow pattern entering the propeller blades.

It has been observed that hull is more efficient when attached to a propeller instead of being towed without propeller the open water efficiency analyses of DTMB 4119 and INSEAN 1619 have been carried out and validated with B-series propeller open water efficiency experimental data.

Effective power and Delivered power values of DARPA Suboff at various velocities were analyzed and results were matched with published data and it was found in good agreement.

Use of COMSOL Multiphysics was helpful in assessment of the flow patterns, in limited time domain, with lot of accuracy. Wake envelop increased as we move from tail to rudder which is why propeller plane near the rudder showed less power requirements

From the above study it can be concluded that the locations away from rudder, revokes the advantage of low velocity region resulting in poor hull efficiency (η_h)

As the location ratio (x/L) is increased, propeller requires more power (P_D) to generate same amount of thrust

Lastly, it is concluded that during the design process, propeller location study shall be carried out to gain maximum propulsive efficiency. As the worst-case scenario design for this DARPA Suboff can cost additional 20% energy penalty, (if propeller is placed randomly at the tail)

CHAPTER 6 – FUTURE WORK

Propulsion System Designing is the specialist domain and shall be included at the very early stage of design. Results of this research mainly emphasis that the designing of Aft Cone, sail and appendages shall be aligned with the propulsor at the concept design level to achieve the maximum propulsive efficiency. This will automatically increase the submerged endurance. Or the capability of platform to carry more payload.

Propeller location survey is a must for each platform that is planned to be designed, as this will vary for each platform.

REFERENCES

[1] "Oceanservice," [Online]. Available: https://oceanservice.noaa.gov/facts/oceandepth.html. [Accessed 12 2021].

[2] E. V. K. Salimzhan A. Gafurov*, "Autonomous unmanned underwater vehicles development tendencies," *Procedia Engineering-ELSEVIER,* 2015.

[3] B. a. Rydel, Concepts in Submarine Design.

[4] D. Watson, Practical Ship Design, Scotland: ELSEVIER-Ocean Engineering Books, 2002.

[5] H. K. Woud and D. Stapersma, Design of Propulsion and Electric Power Generator Systems. , IMarEST, 2003.ISBN 1-902536-47-9.Delft University of Technology, Delft, Netherland, 2002.

[6] Multiple Chinese Authors, Propulsion System Design, 2015.

[7] M. E. R. e. al, "Offshore propulsion: powering the offshore industry," *Marine Engineers,* 2018.

[8] ,. J. T. Ligtelijn, "The pay-off between cavitation and efficiency. Proceedings of the Institute of Marine Engineering, Science & Technology (IMarEST) Ship Propulsion Systems Symposium 2010, London, UK," in *IMAREST*, London, UK, 2010.

[9] "BV Rules for Naval Platforms," 2011.

[10] J. J. K. E. S. Poul Andersen, "Aspects of Propeller Developments for a Submarine," in *First International Symposium on Marine Propulsors*, Trondheim, 2009.

[11] K. M. Flood, "Propeller performance analysis using lifting line theory," Cambridge Massachusetts Institute of Technology, 2009.

[12] P. M. C. Nathan Chase, "Submarine propeller computations and application to self-propulsion," *Ocean Engineering-ELSEVIER,* 2013.

[13] Z. S. L. ZHANG Nan, "Numerical simulation of hull/propeller interaction of submarine in submergence," *Journal of Hydrodynamics-ELSEVIER,* 2013.

[14] M. C. Ö. F. Ç. Yasemin Arıkan Özden, "Numerical Investigation of Submarine Tail Form on the Hull Efficiency," in *Fifth International Symposium on Marine Propulsors*, Finland, 2017.

[15] Florian Vesting, Rickard E. Bensow , Rikard Johansson , Robert Gustafsson, "Procedure for Application-Oriented Optimisation of Marine Propellers," *Journal of Marine Science and Engineering,* 2016.

[16] A. Y. G. Y. A. Ö. T. G. C. M. Cansın Özdena, "Underwater radiated noise prediction for a submarine propeller in different," *Ocean Engineering-ELSEVIER,* 2016.

[17] A. P. a. E. Balaras, "A numerical investigation of the wake of an axisymmetric body with appendages," *Fluid Mechanics ,* 2016.

[18] M. m. e. al., "Evaluation of submairne model test in Toing Tank and comaprison with CFD and Experimental formulas for fully submerged resistance," *Indian Journal of Geo-Marine Sciences,* 2013.

[19] D. E. &. E. Milanov, "Hydrodynamics of DARPA SUBOFF Submarine at Shallowly Immersion Conditions," *International Journal of Marine Navigation & Safety of Sea Transportation,* 2019.

[20] T.-L. L. a. D.-T. Hong, "Computational Fluid Dynamics Study of the Hydrodynamic Characteristics of a Torpedo-Shaped Underwater Glider," *Fluids-MDPI,* 2021.

[21] M. R. M. H. A. K. E. H. M Faizal Ahmad, "Numerical study on drag and lift coefficients of a marine riser at high Reynolds number using COMSOL multiphysics," in *2nd International Conference on Civil & Environmental Engineering*, 2020.

[22] Z. I. M. G. G. S. D. K. Setyo Leksono, "DESIGNING PROPELLER OF MINISUBMARINE 22 M BY USING STANDARD SERIES DATA," *INTERNATIONAL JOURNAL OF ENGINEERING SCIENCES & RESEARCH TECHNOLOGY,* 2018.

[23] A. D. C. D. S. B. Savas Sezen, "Investigation of self-propulsion of DARPA Suboff by RANS method," *Ocean Engineering,* 2018.

[24] S. S. S. B. Cihad Delen, "COMPUTATIONAL INVESTIGATION OF SELF PROPULSION PERFORMANCE OF DARPA SUBOFF VEHICLE," *Tamap Journal of Engineering,* 2017.

[25] S. EKINCI, "A Practical Approach for Design of Marine Propellers with Systematic Propeller Series," *BRODOGRANDNJ,* 2012.

[26] F. D. F. ,. M. F. F. S. M. V. Andrea Pecoraro, "An improved wake description by higher order velocity statistical moments for single screw vessel," *Ocean Engineering-ELSEVIER,* 2015.

[27] Z. J. H. X. Y. D. a. P. H. Zhihui Jin, "Validation of Numerical Simulation on the Flow Field of Submarine with Various Types of stern appendages," *IEEE,* 2018.

[28] O. K. K. e. al., "ON SELF-PROPULSION ASSESSMENT OF MARINE VEHICLES," *Brodogradnja,* 2018.

[29] N. N. Mashud Karim, "Numerical Study on Flow Around Modern Ship Hulls with Rudder-Propeller Interactions," *Journal of Marine Science and Application,* 2019.

[30] S. S. ,. M. A. ,. O. T. Dogancan Uzun, "Effect of biofouling roughness on the full-scale powering performance of a submarine," *Ocean Engineering-ELSEVIER,* 2021.

[31] M. T. Q. M. A.-H. a. R. D. Ruben J. Paredes, "Numerical Flow Characterization around a Type 209 Submarine Using OpenFOAM," *Fluids-MDPI,* 2021.

[32] *. C. D. b. A. D. c. M. A. Savas Sezen a, "An investigation of scale effects on the self-propulsion characteristics of a Submarine," *Applied Ocean Research-ELSEVIER,* 2021.

[33] E. V. K. Salimzhan A. Gafurov, "Autonomous unmanned underwater vehicles development tendencies," *Procedia Engineering-ELSEVIER,* 2015.

[34] J. Carlton, Marine Propellers.

[35] "World Biggest Subamarines," [Online]. Available: https://www.naval-technology.com/features/feature-the-worlds-biggest-submarines/. [Accessed 28 November 2021].

[36] H.-L. L. a. T. T. Huang, "Summary of DARPA Suboff Experimental Program Data," US NAVY, 1998.

[37] ITTC, *1978-Performance Prediction Method,* ITTC, 2008.

[38] ITTC-7.5-03-03-02, *Practical Guidelines for RANS Calculation of Nominal Wakes,* 2014.

[39] F. M. White, Fluid Mechanics Chapter 07 Section 7.4.

[40] ITTC, "ITTC Report of Resistance Committee," in *Proceedings of 8th ITTC, 1957*, Madrid, Spain, 1957.

[41] M. Renilson, Submarine Hydrodynamics, Springer.

[42] W. Frei, "COMSOL," [Online]. Available: https://www.comsol.com/blogs/which-turbulence-model-should-choose-cfd-application/. [Accessed 28 Jul 2021].

[43] D.C. Wilcox, " Turbulence Modeling for CFD, 2nd ed.,," DCW Industries, 1998.

[44] [Online]. Available: https://www.comsol.com/support/knowledgebase/1270. [Accessed December 2021].

[45] D. R. a. P. K. M M. Brintas, "Kt, KQ and Efficiecny Curves for Weigneinian B-series Propellers," University of Michigen, Michigen, USA, 1981.